

A POLAROGRAPHIC INVESTIGATION OF THE REDUCTION
MECHANISM OF CERTAIN COBALT (III) COMPLEX IONS

by

Richard Lee White

Thesis submitted to the Faculty of the
Virginia Polytechnic Institute
in candidacy for the degree of
MASTER OF SCIENCE
in
CHEMISTRY

May 1962

Blacksburg, Virginia

LD
5655
V855
1962
W495
c.2

ACKNOWLEDGMENT

I should like to express my appreciation to Dr. John G. Mason for directing this research and to the other members of the Department for their cooperation and assistance when necessary.

I should also like to express my appreciation to the Research Corporation for financial support rendered during my tenure as a graduate student.

To my wife and my mother-in-law, without whose constant encouragement and sacrifice this would never have been possible.

Table of Contents

	<u>Page</u>
INTRODUCTION	1
NOMENCLATURE	4
HISTORICAL	5
POLAROGRAPHIC METHODS	11
RESULTS AND DISCUSSION	16
EXPERIMENTAL	71
CONCLUSIONS	81
BIBLIOGRAPHY	83
VITA	85

Table of Tables

	<u>Page</u>
Table 1. pH variation on <u>trans</u> $[\text{Co}(\text{en})_2(\text{NO}_2)_2]\text{NO}_3$ phosphate buffer	17
Table 2. pH variation on <u>trans</u> $[\text{Co}(\text{en})_2(\text{NO}_2)_2]\text{NO}_3$ in borate buffer	18
Table 3. Nitrite variation on <u>trans</u> - $[\text{Co}(\text{en})_2(\text{NO}_2)_2]\text{NO}_3$ in phosphate buffer	20
Table 4. Nitrite variation on <u>trans</u> - $[\text{Co}(\text{en})_2(\text{NO}_2)_2]\text{NO}_3$ in borate buffer	21
Table 5. Nitrite variation on <u>trans</u> - $[\text{Co}(\text{en})_2(\text{NO}_2)_2]\text{NO}_3$ in borate buffer	22
Table 6. Ammonium variation on <u>trans</u> - $[\text{Co}(\text{en})_2(\text{NO}_2)_2]\text{NO}_3$ in acetate buffer	27
Table 7. pH variation on <u>cis</u> - $[\text{Co}(\text{en})_2(\text{NCS})_2]\text{NCS}$ in phosphate buffer	31
Table 8. pH variation on <u>cis</u> - $[\text{Co}(\text{en})_2(\text{NCS})_2]\text{NCS}$ in borate buffer	32
Table 9. Thiocyanate variation on <u>cis</u> - $[\text{Co}(\text{en})_2(\text{NCS})_2]\text{NCS}$ in phosphate buffer	34
Table 10. pH variation on $[\text{Co}(\text{en})_2(\text{C}_2\text{O}_4)] \text{Cl}$ in phosphate buffer	39
Table 11. pH variation on $[\text{Co}(\text{en})_2(\text{C}_2\text{O}_4)] \text{Cl}$ in borate buffer	40
Table 12. pH variation on <u>cis</u> $[\text{Co}(\text{dipy})_2(\text{NO}_2)_2]\text{Cl}$ in phosphate buffer	45
Table 13. pH variation on <u>trans</u> $[\text{Co}(\text{en})_2(\text{NO}_2)_2]\text{NO}_3$ in phosphate buffer at the platinum electrode	53
Table 14. pH variation on <u>cis</u> $[\text{Co}(\text{en})_2(\text{NCS})_2]\text{NCS}$ in phosphate buffer at the platinum electrode	55

Table of Tables (Continued)

	<u>Page</u>
Table 15. pH variation on $[\text{Co}(\text{en})_2(\text{C}_2\text{O}_4)]\text{Cl}$ in phosphate buffer at the platinum electrode	57
Table 16. pH variation on <u>cis</u> $[\text{Co}(\text{dipy})_2(\text{NO}_2)_2]\text{Cl}$ in phosphate buffer at the platinum electrode	60
Table 17. pH variation on <u>cis</u> $[\text{Co}(\text{dipy})_2(\text{NO}_2)_2]\text{Cl}$ in acetate buffer at the platinum electrode	61
Table 18. pH variation on $[\text{Co}(\text{dipy})_2(\text{C}_2\text{O}_4)]\text{Cl}$ in phosphate buffer at the platinum electrode	63
Table 19. pH variation on $[\text{Co}(\text{dipy})_2(\text{C}_2\text{O}_4)]\text{Cl}$ in acetate buffer at the platinum electrode	64
Table 20. pH variation on <u>trans</u> $[\text{Co}(\text{phen})_2(\text{NO}_2)_2]\text{NO}_3$ in phosphate buffer at the platinum electrode	66
Table 21. pH variation on <u>trans</u> $[\text{Co}(\text{phen})_2(\text{NO}_2)_2]\text{NO}_3$ in acetate buffer at the platinum electrode	67
Table 22. Comparison of $E_{1/2}$ at the D.M.E. and the platinum electrode	69

Table of Figures

	<u>Page</u>
Figure 1. Ir versus $[\text{OH}^-]$ for <u>trans</u> $[\text{Co}(\text{en})_2(\text{NO}_2)_2]\text{NO}_3$	19
Figure 2. $E_{1/2}$ versus $\log [\text{NO}_2^-]$ for <u>trans</u> - $[\text{Co}(\text{en})_2(\text{NO}_2)_2]\text{NO}_3$	23
Figure 3. Polarogram for <u>trans</u> $[\text{Co}(\text{en})_2(\text{NO}_2)_2]\text{NO}_3$	24
Figure 4. Slope analysis for the first wave of <u>trans</u> $[\text{Co}(\text{en})_2(\text{NO}_2)_2]\text{NO}_3$	25
Figure 5. Ir versus $[\text{OH}^-]$ for <u>cis</u> $[\text{Co}(\text{en})_2(\text{NCS})_2]\text{NCS}$	33
Figure 6. $E_{1/2}$ versus $\log [\text{NCS}^-]$ for <u>cis</u> - $[\text{Co}(\text{en})_2(\text{NCS})_2]\text{NCS}$	35
Figure 7. Polarogram for <u>cis</u> $[\text{Co}(\text{en})_2(\text{NCS})_2]\text{NCS}$	36
Figure 8. Ir versus $[\text{OH}^-]$ for $[\text{Co}(\text{en})_2(\text{C}_2\text{O}_4)]\text{Cl}$	41
Figure 9. Polarogram for $[\text{Co}(\text{en})_2(\text{C}_2\text{O}_4)]\text{Cl}$	42
Figure 10. $E_{1/2}$ versus pH for the second wave of the three ethylenediamine complexes	43
Figure 11. Ir versus $[\text{OH}^-]$ for <u>cis</u> - $[\text{Co}(\text{dipy})_2(\text{NO}_2)_2]\text{Cl}$	46
Figure 12. Polarogram for <u>cis</u> $[\text{Co}(\text{dipy})_2(\text{NO}_2)_2]\text{Cl}$	47
Figure 13. Polarogram for $[\text{Co}(\text{dipy})_2(\text{C}_2\text{O}_4)]\text{Cl}$	49
Figure 14. Polarogram for $\text{Na}[\text{Co}(\text{EDTA})(\text{NO}_2)]$	51
Figure 15. Polarogram for <u>trans</u> $[\text{Co}(\text{en})_2(\text{NO}_2)_2]\text{NO}_3$ at the platinum electrode	54
Figure 16. Polarogram for <u>cis</u> $[\text{Co}(\text{en})_2(\text{NCS})_2]\text{NCS}$ at the platinum electrode	56
Figure 17. Polarogram for $[\text{Co}(\text{en})_2(\text{C}_2\text{O}_4)]\text{Cl}$ at the platinum electrode	58

Table of Figures (Continued)

	<u>Page</u>
Figure 18. Polarogram for <u>cis</u> $[\text{Co}(\text{dipy})_2(\text{NO}_2)_2]\text{Cl}$ at the platinum electrode	62
Figure 19. Polarogram for $[\text{Co}(\text{dipy})_2(\text{C}_2\text{O}_4)]\text{Cl}$ at the platinum electrode	65
Figure 20. Polarogram for <u>trans</u> $[\text{Co}(\text{phen})_2(\text{NO}_2)_2]\text{NO}_3$ at the platinum electrode	68

INTRODUCTION

The study of complex ion reactions for the purpose of describing the mechanism of the reaction and relating structure to mechanism has been mainly confined to substitution reactions of complexes which are not in rapid equilibrium with the complexing ligand.

Polarographic reduction studies have dealt mainly with metal complexes which are substitutionally labile and which exhibit reversible behavior at the dropping mercury electrode.

Some studies have been made of complexes in which the oxidized and reduced forms of the complex are both inert, by the classification of Taube (1). Studies have been made of complexes of the Co(III)-Co(II) system by Tsuchida (2), Holtzclaw (3), and others, but little effort has been made to describe the mechanism and its relation to structure.

The polarographic reduction of Co(III) complexes to Co(II) involves a change in electronic configuration, dependent on the nature of the ligand. Co(III) exhibits a d^2sp^3 inner orbital configuration while Co(II) exhibits an inner orbital sp^3d^2 , or an sp^3d configuration for the five-coordinated $Co(CN)_5^{-3}$ proposed by Adamson (4). This change in configuration upon reduction results in substitutional lability for Co(II) complexes in general. Since the bond distances are changed, rapid electron exchange cannot be achieved and these systems generally appear to be irre-

versibly reduced polarographically. Certain cobalt complexes do show polarographically reversible behavior. Laitinen and Grieb (5) report reversibility of the $[\text{Co}(\text{en})_3]^{3+} - [\text{Co}(\text{en})_3]^{2+}$ system in excess ethylenediamine and Kivalo (6) reports that $[\text{Co}(\text{en})_3]^{3+}$ is polarographically reversible in the absence of excess ethylenediamine. Dolezal (7) though, reports that this system is not perfectly reversible. The apparent reversibility of this and other cobalt complexes is brought about by the high ligand field of the complexing ligands which cause Co(II) to become spin paired as is Co(III).

There is evidence that with certain ligands, Co(II) may have a coordination number of five. Five-coordinated cobalt complexes have been reported by Adamson (4) and by Nyholm (8) for CN^- and NO_2^- respectively. For most other ligands, such as NH_3 , a coordination number of six is indicated.

The irreversibility of most cobalt complex reductions may be attributed to the slow orbital rearrangement from d^2sp^3 to a sp^3d^2 configuration following the one electron reduction step, the electronic rearrangement being the rate determining step. When the complex contains ligands of high spin-pairing ability, such as NO_2^- , it has been suggested that a five-coordinated Co(II) species with a dsp^3 configuration, could, upon oxidation, be more easily converted to a d^2sp^3 configuration without a high activation

energy being involved. The proposed five-coordinated Co(II) complex could thus show reversible electrochemical behavior.

The observation of Mason (9), with respect to the reversibility of the $[\text{Co}(\text{en})_2(\text{NO}_2)_2]\text{NO}_3$ system suggests that since NO_2^- and ethylenediamine are both effective spin-pairing ligands, a species $[\text{Co}(\text{en})_2\text{NO}_2]^+$ has a finite existence at the electrode surface, and reversibility is a function of spin-pairing ability.

The purpose of this investigation was to determine the polarographic behavior and pH dependance of the polarographic reduction of bis-(dipyridyl) and bis-(orthophenanthroline)-dinitro complexes of cobalt (III). These complexes should show reversibility if the hypothesis is true. The complexes $[\text{Co}(\text{en})_2(\text{C}_2\text{O}_4)]^+$, $[\text{Co}(\text{en})_2(\text{NCS})_2]^+$, $[\text{Co}(\text{dipy})_2(\text{C}_2\text{O}_4)]^+$, $[\text{Co}(\text{EDTA})\text{NO}_2]^-$ and $[\text{Co}(\text{EDTA})\text{Br}]^-$ selected because of the difference in spin pairing ability of thiocyanate and oxalate, as compared to nitrite, and because of the differences between ethylenediamine and ethylenediaminetetraacetate.

NOMENCLATURE

- en ▪ ethylenediamine
- dipy ▪ α, α' -dipyridyl
- phen ▪ orthophenanthroline
- EDTA ▪ ethylenediaminetetraacetate
- $E_{1/2}$ ▪ half wave potential, in volts, versus the saturated calomel cell
- S.C.E. ▪ saturated calomel cell (reference cell)
- i_1 ▪ limiting current of the first reduction wave, in microamperes
- i_d ▪ total diffusion current of the reduction, in microamperes
- I_r ▪ the ratio of the height of the first reduction wave to the total wave height
- D.M.E. ▪ dropping mercury electrode

HISTORICAL

Electron transfer reactions occur readily in the gaseous phase, but in the liquid phase, electron transfer becomes hindered by the close proximity of the solvent molecules, or other ions in solution, to the molecule or atom undergoing electron exchange. Marcus ⁽¹⁰⁾ concluded that the important factors which determine the speed of an electron transfer reaction in solution are; the standard free-energy change of the rate determining step, the coulombic interaction of ionic charges of the reactants, and the solvation of the charged reactants. Irvine ⁽¹¹⁾, in an investigation of the persulfate oxidation of Fe(II) complexes, confirmed the Marcus hypothesis and suggested that the overall free-energy change may be of some importance also.

Certain metal complexes have been established ⁽¹²⁾ as undergoing electron-transfer reductions. These include $[\text{Fe}(\text{CN})_6]^{3-}$, $[\text{Fe}(\text{phen})_3]^{3+}$, $[\text{Fe}(\text{dipy})_3]^{3+}$, $[\text{Co}(\text{phen})_3]^{3+}$ and $[\text{Co}(\text{dipy})_3]^{3+}$. In these cases, both the oxidized and the reduced forms are essentially inert to rapid substitution in the coordination sphere, and interpenetration, required for atom transfer, is essentially ruled out.

For most cobalt (III) complexes, the oxidized species is inert while the reduced form is labile, which means that upon reduction, the complex undergoes ligand exchange with the solvent or other ions in solution. This substitution complicates, considerably, the proposal of a mechanism for the reduction.

From a study of the reduction of $[\text{Co}(\text{NH}_3)_6]^{3+}$, by Laitenen and Kivalo ⁽¹³⁾, an explanation of the irreversibility of the reduction was proposed as the slow electronic orbital rearrangement from a d^2sp^3 to an sp^3d^2 configuration. It was proposed that the one-electron reduction was followed by the slow, rate-determining, orbital rearrangement step. When ethylenediamine was present, the reduction of $[\text{Co}(\text{NH}_3)_6]^{3+}$ showed a single reversible wave, the half-wave potential of which corresponded to the $[\text{Co}(\text{en})_3]^{3+} - [\text{Co}(\text{en})_3]^{2+}$ couple. This was attributed to: first, the reduction of $[\text{Co}(\text{NH}_3)_6]^{3+}$ to $[\text{Co}(\text{NH}_3)_6]^{2+}$; second, the ligand exchange of the ethylenediamine for ammonia; third, the oxidation of the $[\text{Co}(\text{en})_3]^{2+}$ to $[\text{Co}(\text{en})_3]^{3+}$; and fourth, at more negative potentials, the reduction of the $[\text{Co}(\text{en})_3]^{3+}$. At potentials more positive than -0.465 volts, versus the saturated calomel reference electrode, the net current will be zero.

The polarographic reduction of $[\text{Co}(\text{en})_3]^{3+}$ in absence of excess ethylenediamine shows an irreversible wave. Kivalo ⁽¹⁴⁾, though, has shown that the reduction is polarographically reversible, and that the irreversible wave is due to the decomposition of the reduced species into lower amines, altering the half-wave potential and the shape of the wave.

Laitenen and Grieb (15) have shown that the reduction of $[\text{Co}(\text{en})_3]^{3+}$ gives a reversible polarographic wave in the presence of excess ethylenediamine. The oxidation of $[\text{Co}(\text{en})_3]^{2+}$, in excess ethylenediamine, shows reversible behavior as well. As the concentration of ethylenediamine is reduced below 0.005M (for a 0.001M $[\text{Co}(\text{en})_3]^{3+}$ concentration), the wave becomes irreversible.

Double reduction waves have been reported for cobalt amine by several writers. Holtzclaw and Sheetz (16) reported double reduction waves for a series of cobalt complexes containing one or two negative ligands. The explanation for the double wave was proposed as being due to an aquated species in equilibrium with the parent compound. The proposed aquo compounds show more negative half-wave potentials than the parents. The evidence given for the presence of an aquo species is that the second wave of all the compounds shows a half-wave potential at about -0.40 volts (versus saturated calomel electrode).

The cobalt complexes of the series studied by Holtzclaw and Sheetz had a bis-ethylenediamine core with various negative monodentate ligands completing the coordination shell. Certain of these complexes, though, do not aquate rapidly enough to account for the height of the reported second wave. The fact that trans $[\text{Co}(\text{en})_2(\text{NO}_2)_2]\text{NO}_3$ and $[\text{Co}(\text{en})_2(\text{NCS})_2]\text{NCS}$ are prepared

in hot aqueous solution and are purified by recrystallization from hot water in high yield indicates that only negligible aquation would take place in cool aqueous solution of these compounds.

The complexes studied by Holtzclaw and Sheetz were in unbuffered solution with KCl as the supporting electrolyte. In an unbuffered solution, the reduction product, being labile, would decompose, releasing free ethylenediamine, thereby altering the pH of the solution in the vicinity of the electrode. This could account for the irreversibility of the observed wave.

In a study of trans-dinitro bis-(ethylenediamine) cobalt (III) nitrate by Mason ⁽¹⁷⁾, the reduction in well-buffered solution gave an apparently reversible wave. In alkaline solution, two waves were produced. The first wave was reversible and the half-wave potential was found to be dependent on nitrite ion concentration but independent of pH. The second wave was irreversible, the half-wave potential was dependent on pH and independent of nitrite ion concentration. The height of the first wave was dependent on pH but the total wave height was dependent only on the concentration of complex. From these, and other considerations, the proposed mechanism was a rapid reversible electron transfer, followed by a decomposition of the reduced species, then the subsequent oxidation of the decomposition product.

A series of complexes studied by Vlcek (18) showed a relation between the half wave potential and the spectroscopic series of the complexes. The complexes studied were of the form $[\text{Co(III)}(\text{NH}_3)_5\text{X}]$ and $[\text{Co(III)}(\text{CN})_5\text{X}]$ where X was either neutral or negative. The spectroscopic series discussed here derives from the difference between the absorption in the spectra of the particular complex and the parent complex $[\text{Co(III)Y}_6]$. Vlcek obtained a straight line plot of $\Delta\nu$ versus $E\frac{1}{2}$ for series of compounds where X was neutral, negative, or doubly negative.

Tsuchida (19) studied a series of Co(III) complexes of the form $[\text{Co}(\text{en})_2\text{X}_2]^+$ and $[\text{Co}(\text{en})_2\text{Y}]^+$ where X and Y were negative and doubly negative ligands, respectively. The stability of these complexes did not agree with the spectroscopic series.

From a study of the reduction of Co(II), in the presence of excess CN^- , Kolthoff and Hume (20) found the reduction to be irreversible and to require one electron per mole of Co(II). When $\text{K}_3[\text{Fe}(\text{CN})_6]$ was added to a solution of CoCl_2 in KCN, it was found that one mole of $[\text{Fe}(\text{CN})_6]^{3-}$ was reduced per mole of Co to produce an oxidation product which was reducible, at the mercury drop, at about the same potential as $[\text{Co}(\text{CN})_5(\text{H}_2\text{O})]^{2-}$. From these observations and the fact that $[\text{Co}(\text{CN})_6]^{3-}$ is not reducible in this medium, they concluded that the Co(II), in excess CN^- , forms $[\text{Co}(\text{CN})_5(\text{H}_2\text{O})]^{3-}$, which may be oxidized to $[\text{Co}(\text{CN})_5(\text{H}_2\text{O})]^{2-}$,

both of which then reduce to complexes of Co(I) which are not oxidizable or reducible at the mercury drop.

POLAROGRAPHIC METHODS

The term polarography is defined as the determination of current-voltage waves of solutions of electrooxidizable or electroreducible substances which are electrolysed in a cell in which one electrode consists of a dropping mercury electrode. This definition applies especially when such "polarization curves" are automatically recorded. The term polarography was coined by Jaroslav Heyrovsky (26), who, along with Shikata (27) invented the instrument known as the polarograph. Kolthoff and Laitinen (28) advocated the name voltammetry to indicate that voltage and current are the two quantities being measured. The term voltammetry also includes cases in which microelectrodes are used in place of the dropping electrode.

When a solution of an electrooxidizable or electroreducible substance is electrolyzed in a polarographic cell, the potential is changed at a constant rate, with respect to an external reference cell, usually a saturated calomel electrode (S.C.E.). The recorded current is zero, or nearly so in the potential region prior to the electrolysis. As the externally applied potential approaches that of the electrochemical reaction of the substance in solution, the current increases. This increase in current continues as the potential changes, then becomes constant, or nearly so. This constant current region is caused by the electrochemical reaction of all reactant in the vicinity

of the electrode surface. The electrode is thus concentration polarized and the current can no longer increase because it is determined by the rate of diffusion of the reacting substance from the bulk of the solution to the electrode surface. The potential which corresponds to a current, on the current-voltage curve, equal to one-half the limiting current is known as the half-wave potential ($E_{1/2}$). The potential of a reversible redox reaction, at the dropping mercury electrode, for a simple metal ion being reduced to a lower oxidation state obeys the equation:

$$E_{d.e.} = E^{\circ} - \frac{RT}{nF} \ln \frac{C_{red.}^{\circ} f_{red.}}{C_{ox.}^{\circ} f_{ox.}} \quad (I)$$

where $C_{red.}^{\circ}$ and $C_{ox.}^{\circ}$ are the concentrations of the metal ions in the lower and higher oxidation states at the electrode surfaces, $f_{red.}$ and $f_{ox.}$ are the corresponding activity coefficients, and E° is the ordinary formal potential of the reaction. As the concentration of the reduced form of the metal is zero, originally, we may assume that the concentration of the reduced form produced at the electrode surface at any point of the wave will be directly proportional to the current:

$$C_{red.}^{\circ} = k' i = \frac{i}{k_{red.}} \quad (II)$$

where $k_{red.}$ is proportional to the square root of the diffusion coefficient of the reduced form. Also:

$$C_{ox.}^{\circ} = k'(i_d - i) = \frac{i_d - i}{k_{ox.}} \quad (III)$$

Substituting for C_{ox}^0 and C_{red}^0 in (I) above:

$$E_{d.e.} = E^0 - \frac{RT}{nF} \ln \frac{f_{red.} k_{ox.}}{f_{ox.} k_{red.}} - \frac{RT}{nF} \ln \frac{i}{i_d - i} \quad (IV)$$

At the half-wave potential, $i = i_d/2$ so

$$E_{\frac{1}{2}} = E^0 - \frac{RT}{nF} \ln \frac{f_{red.} k_{ox.}}{f_{ox.} k_{red.}} \quad (V)$$

and substituting in (I) above, we have:

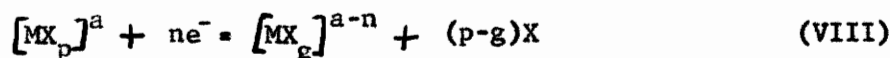
$$E_{d.e.} = E_{\frac{1}{2}} - \frac{RT}{nF} \ln \frac{i}{i_d - i} \quad (VI)$$

and at 25° C. this reduces to:

$$E_{d.e.} = E_{\frac{1}{2}} - \frac{.0591}{n} \log \frac{i}{i_d - i} \quad (VII)$$

where (i_d) is the limiting current and (n) corresponds to the number of electrons exchanged, it becomes evident that a graph of $E_{d.e.}$ versus $\log i/(i_d - i)$ should produce a straight line with a slope of $0.0591/n$ and the potential where the log term becomes zero should be the $E_{\frac{1}{2}}$.

In the case of complex metal ions which are reduced reversibly from one oxidation state to another, the net electrode reaction take the form:



the potential at any point on the wave is then expressed by:

$$E_{d.e.} = E^0 - \frac{0.0591}{n} \log \frac{C_{red}^0 (C_x)^{p-g}}{C_{ox}^0} \quad (IX)$$

where C_{red}^0 and C_{ox}^0 represent the concentrations of MX_p and MX_g

respectively and C_x is the concentration of the ligand. This equation assumes; a reversible electrode reaction, sufficient electrolyte so that current is entirely diffusion controlled, and sufficient excess of the complexing ligand such that the ligand concentration at the electrode surface will be virtually constant. It has been determined that the $E_{\frac{1}{2}}$ in this case, is independent of the concentration of the complex metal ion and dependent on the concentration of the complexing ligand, because at the half-wave potential, $C_{red}^O = C_{ox}^O$, $E_{d,e.} = E_{\frac{1}{2}}$, which then varies only with C_x the concentration of the ligand, assuming activity coefficients are constant for all ions and molecules involved. From the above equation, it is noted that:

$$\frac{E_{\frac{1}{2}}}{\log C_x} = - \frac{0.0591}{n} \quad (p-g) \quad (X)$$

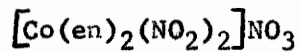
This reaction enables us to determine the coordination number, p , of the complex ion, and thus its formula.

When a rotating platinum electrode is used in place of the dropping mercury electrode, electrode reactions which show reversibility at the D.M.E. tend to show irreversibility at the rotating platinum electrode. In this case, the stirring of the solution by the electrode keeps the concentration of the reacting substance at the electrode surface equal, or nearly so, to its concentration in the bulk of the solution. Under these conditions,

the current depends only on the rate of the electrode reaction and not on the rate of mass transfer to the electrode. The current may be influenced by the catalytic properties of the electrode surface and by slight changes in the area of the electrode surface.

RESULTS AND DISCUSSION

Dropping Mercury Electrode



The half wave potentials and wave heights of the two waves are shown in Table 1 for the reduction in phosphate buffers for pH values of 5.78 to 11.26. The half wave potential of the first wave is seen to be essentially constant while the half wave potential of the second wave is seen to become increasingly more negative as the pH increases. The slope analysis of the first wave, an example of which is shown in Figure 4, shows that the first wave corresponds to a reversible one electron reduction. The apparent reversibility of the second wave is not in agreement with the results obtained by Mason (32).

An example of the double wave may be seen in the polarogram in Figure 3.

Table 2 shows the data from the reduction in borate buffers in the pH range from 7.15 to 11.10. The half wave potential of the first wave is seen to be constant and is essentially the same as in phosphate buffer. The first wave again shows reversible behavior. The second wave varies with pH in much the same manner as in phosphate buffers but the wave is more positive than in phosphate buffer.

Figure 1 shows the variation of the height of the first wave expressed as the ratio of the first limiting current to the total diffusion current in phosphate and in borate buffers.

TABLE 1

The Reduction of 0.001M trans [Co(en)₂(NO₂)₂]NO₃ as a
Function of pH in 0.2M Phosphate Buffer

pH	First Wave			Second Wave			
	<u>E_{1/2}, volts</u>	<u>i₁, μa</u>	<u>Slope</u>	<u>E_{1/2}, volts</u>	<u>i_d, μa (total)</u>	<u>Slope</u>	<u>Ir</u>
5.78	-0.265	4.29	0.0625	-	-	-	-
6.69	-0.265	4.34	0.0620	-	-	-	-
8.20	-0.267	4.19	0.0630	-	-	-	-
9.25	-0.263	3.60	0.0620	-0.466	4.13	0.0600	0.872
9.60	-0.262	3.04	0.0595	-0.462	4.06	0.0595	0.749
10.14	-0.260	3.08	0.0610	-0.472	4.30	0.0585	0.716
10.52	-0.267	2.93	0.0595	-0.489	4.20	0.0610	0.697
10.69	-0.264	2.96	0.0630	-0.497	4.26	0.0605	0.694
11.27	-0.269	2.84	0.0575	-0.516	4.20	0.0600	0.676

TABLE 2

The Reduction of 0.001M $[\text{Co}(\text{en})_2(\text{NO}_2)_2]\text{NO}_3$ as a Function of pH in 0.2M Borate Buffer

pH	First Wave			Second Wave			
	$E_{1/2}$, volts	$i_1, \mu\text{a}$	Slope	$E_{1/2}$, volts	$i_d, \mu\text{a}$ (total)	Slope	Ir
7.15	-0.260	4.06	0.0610	-	-	-	-
8.82	-0.260	3.16	0.0617	-0.372	4.10	0.0605	0.770
9.45	-0.265	2.81	0.0608	-0.405	4.08	0.0598	0.690
9.50	-0.268	2.63	0.0625	-0.414	4.05	0.0625	0.650
10.40	-0.266	2.31	0.0610	-0.412	4.04	0.0615	0.564
10.42	-0.266	2.29	0.0610	-0.422	4.06	0.0620	0.564
10.45	-0.260	2.27	0.0600	-0.430	4.06	0.0600	0.560
11.10	-0.265	2.20	0.0605	-0.435	4.08	0.0610	0.540

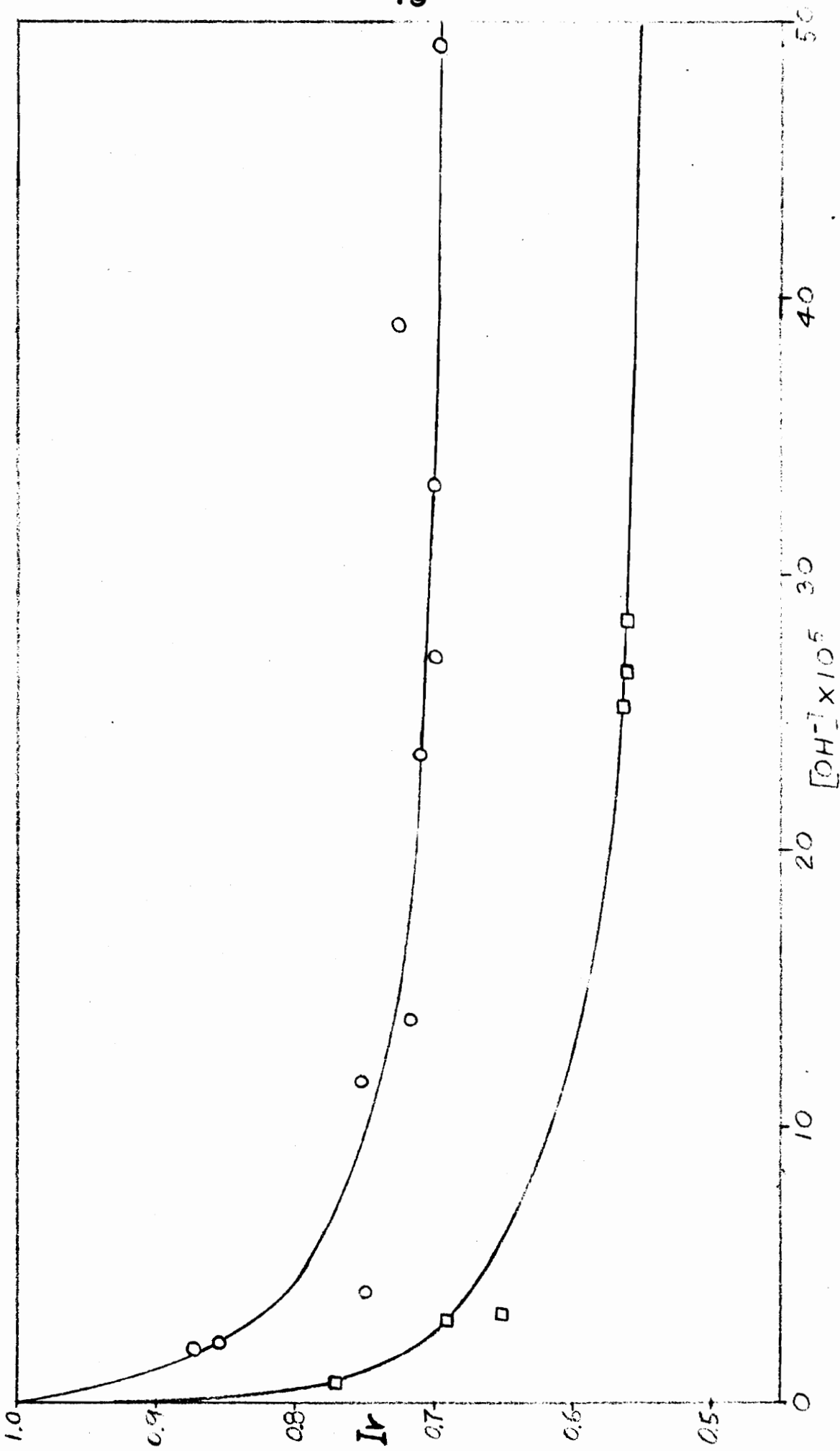


Figure 1

The Relative Height of the First Reduction Wave of $[Co(en)_2(NO_2)_2]NO_3$ as a Function of $[OH^-]$. \circ , Phosphate Buffer; \square , Borate Buffer

TABLE 3

The Reduction of 0.001M trans[Co(en)₂(NO₂)₂]NO₃ as a Function of Nitrite Concentration in 0.2M Phosphate Buffer at pH 10.4

<u>[NO₂⁻],</u> <u>M</u>	<u>First Wave</u>			<u>Second Wave</u>			
	<u>E_{1/2},</u> <u>volts</u>	<u>i₁, μa</u>	<u>Slope</u>	<u>E_{1/2},</u> <u>volts</u>	<u>i_d, μa</u> <u>(total)</u>	<u>Slope</u>	<u>Ir</u>
0	-0.260	2.69	0.0615	-0.476	4.04	0.0610	0.664
0.001	-0.264	2.68	0.0625	-0.469	4.04	0.0600	0.663
0.010	-0.299	2.72	0.0791	-0.481	4.09	0.0615	0.665
0.020	-0.318	2.68	0.0845	-0.480	4.07	0.0605	0.660
0.050	-0.345	2.65	0.0873	-0.470	4.02	0.0630	0.659
0.070	-0.363	2.73	0.0887	-0.482	4.04	0.0705	0.675
0.100	-0.408	4.08	-	-	-	-	1.000

TABLE 4

The Reduction of 0.001M $[\text{Co(en)}_2(\text{NO}_2)_2]\text{NO}_3$ as a Function of Nitrite Concentration in 0.2M Borate Buffer at pH 10.4

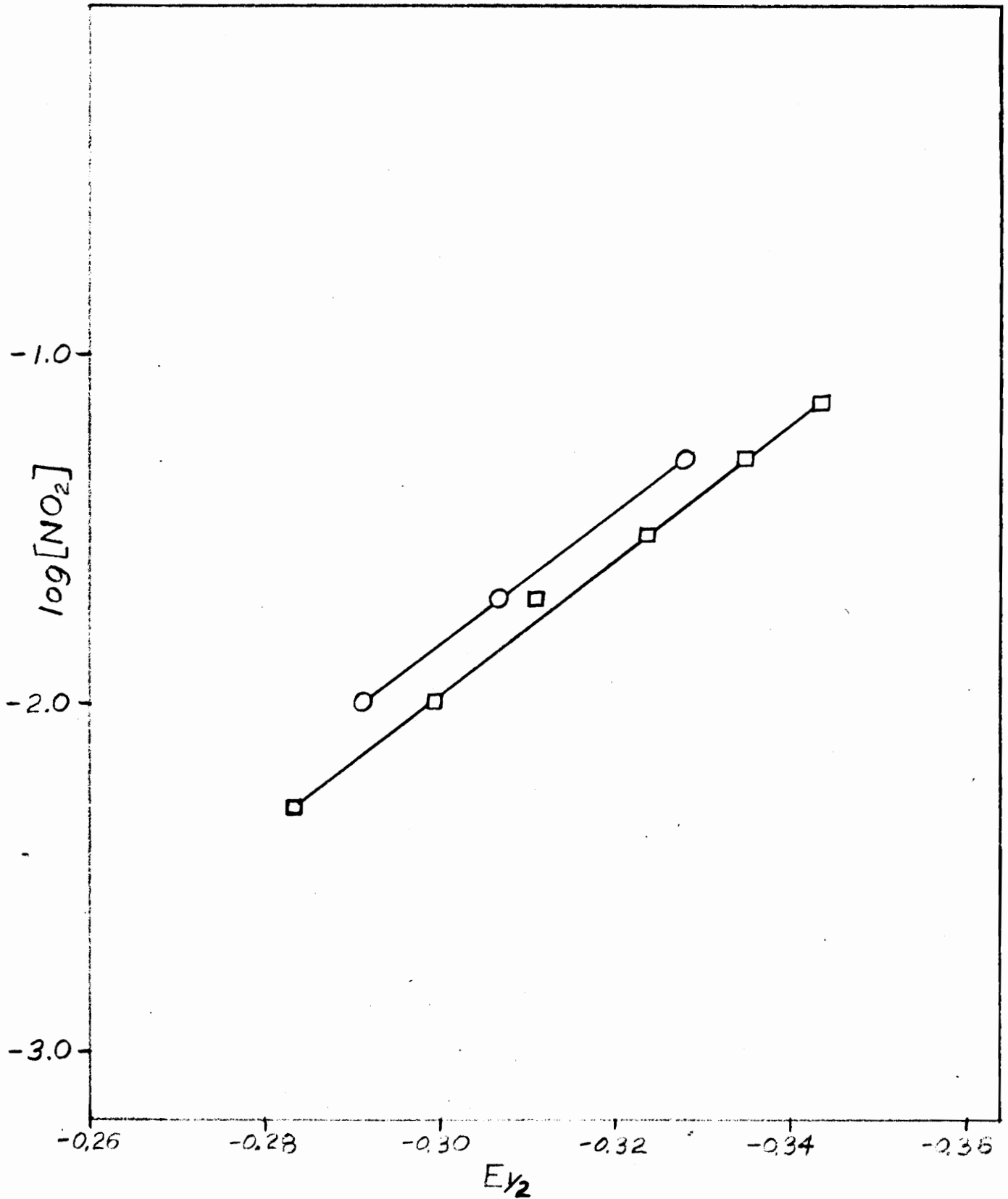
$[\text{NO}_2^-]$, M	First Wave			Second Wave			
	$E_{1/2}$, volts	$i_l, \mu\text{a}$	Slope	$E_{1/2}$, volts	$i_d, \mu\text{a}$ (total)	Slope	Ir
0	-0.266	2.45	0.0651	-0.412	4.34	0.0617	0.565
0.001	-0.270	2.48	0.0605	-0.420	4.34	0.0621	0.572
0.005	-0.279	2.49	0.0597	-0.416	4.34	0.0600	0.574
0.010	-0.299	2.47	0.0602	-0.422	4.35	0.0605	0.568
0.020	-0.313	2.41	0.0618	-0.418	4.29	0.0600	0.562
0.030	-0.329	2.42	0.0622	-0.421	4.28	0.0602	0.566
0.050	-0.343	2.41	0.0598	-0.422	4.30	0.0595	0.561
0.070	-0.354	2.42	0.0603	-0.438	4.29	-	0.564

TABLE 5

The Reduction of 0.001M $[\text{Co(en)}_2(\text{NO}_2)_2]\text{NO}_3$ as a Function of Nitrite Ion Concentration in 0.2M Borate Buffer at pH 9.5

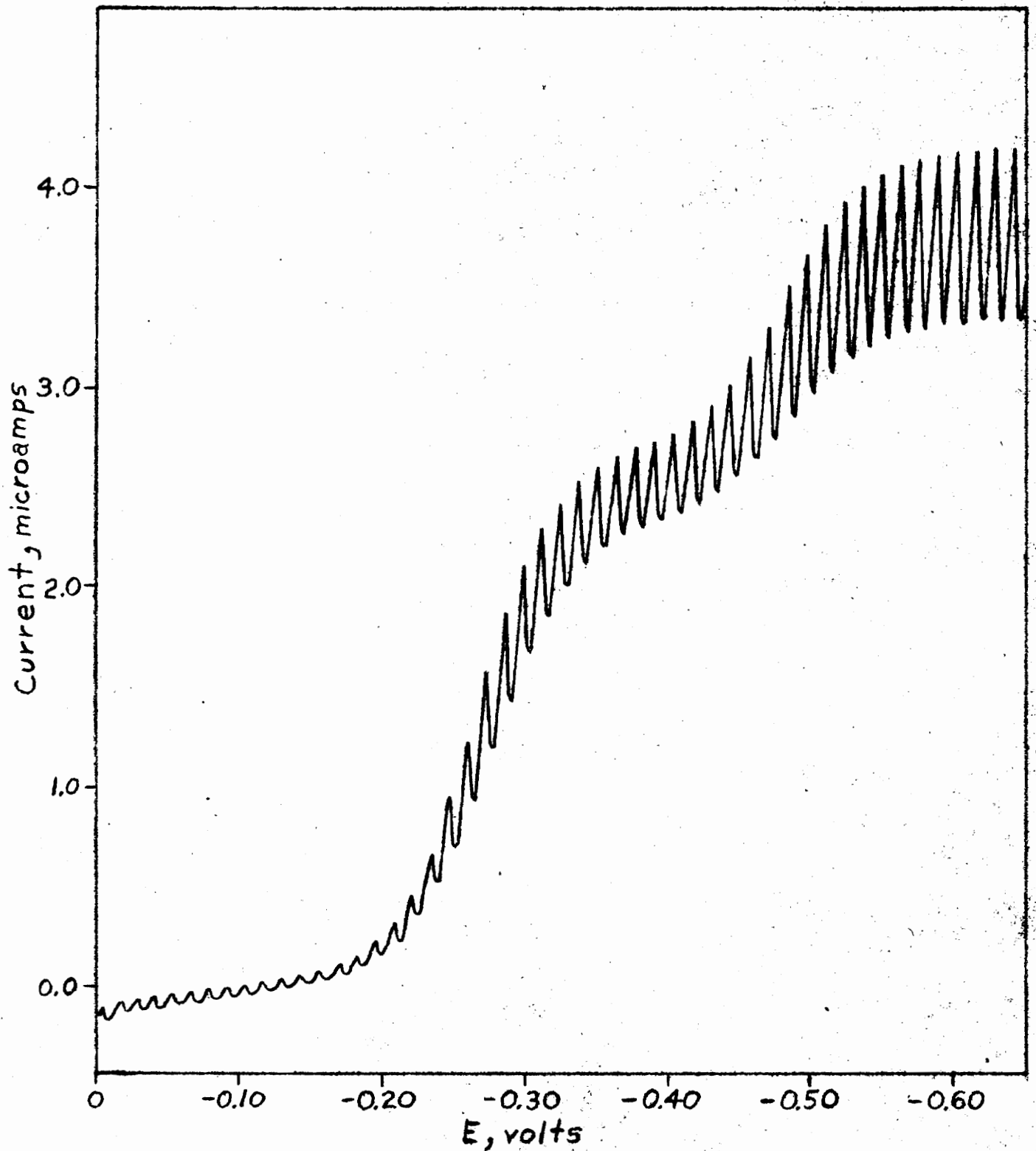
$[\text{NO}_2^-]$, M	First Wave			Second Wave			
	$E_{1/2}$, volts	$i_1, \mu\text{a}$	Slope	$E_{1/2}$, volts	$i_d, \mu\text{a}$ (total)	Slope	Ir
0	-0.268	2.70	0.0623	-0.414	4.16	0.0610	0.649
0.001	-0.272	2.71	0.0620	-0.410	4.19	0.0602	0.646
0.010	-0.293	2.77	0.0608	-0.410	4.27	0.0605	0.647
0.080	-0.379	2.72	0.0605	-0.453	4.23	-	0.642
0.100	-0.388	2.74	0.0603	-0.460	4.25	-	0.645

Figure 2



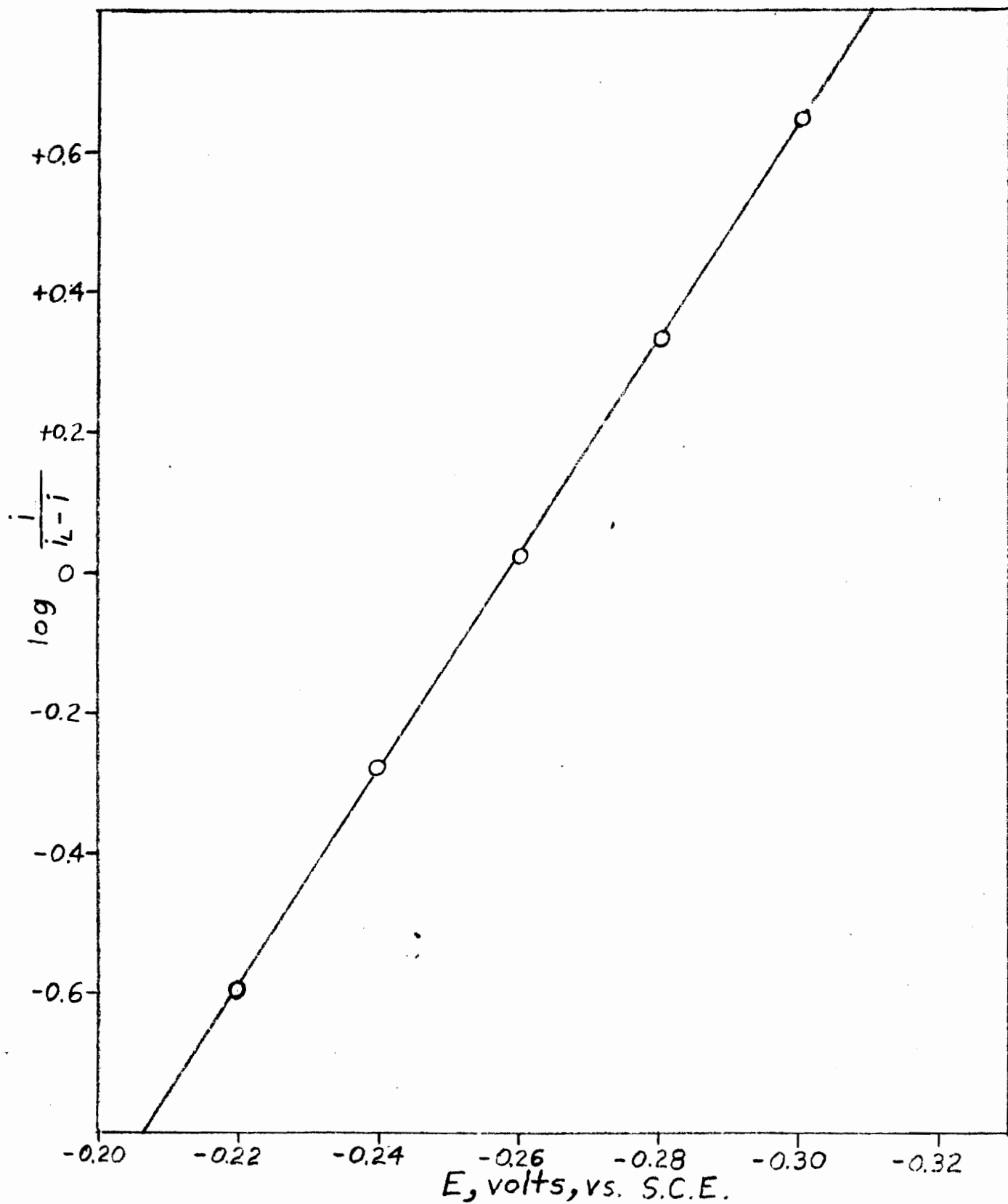
The Half Wave Potential of the First Reduction Wave of $[\text{Co}(\text{en})_2(\text{NO}_2)_2]\text{NO}_3$ as a Function of Nitrite Ion Concentration; in Phosphate; O; in Borate; □

Figure 3



Polarogram of the Reduction of $[\text{Co}(\text{en})_2(\text{NO}_2)_2]\text{NO}_3$ in Phosphate Buffer at pH 10.43

Figure 4

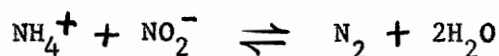


Slope Analysis of the First Reduction Wave for
 $[\text{Co}(\text{en})_2(\text{NO}_2)_2]\text{NO}_3$ in Phosphate Buffer at pH 10.43

Figure 2 shows the change in $E_{\frac{1}{2}}$ of the first wave as a function of nitrite ion concentration in phosphate and in borate buffers. The range of concentrations of nitrite is limited, as high concentrations cause the first wave to merge with the second wave. The magnitude of the shift in $E_{\frac{1}{2}}$ is approximately 0.060 volts for a ten-fold change in nitrite ion concentration. This shift in the $E_{\frac{1}{2}}$ and the magnitude of the shift indicate that one nitrite is released as a part of the primary electrode process. The addition of nitrite ion to the solution shifts the equilibrium of the nitrite releasing reaction, making it more difficult for the nitrite to be released and so show a more negative $E_{\frac{1}{2}}$.

Table 3 gives the data for the reduction as a function of nitrite ion concentration in phosphate buffer at pH 10.4. Tables 4 and 5 show the dependence of the first wave on nitrite ion concentration at pH 10.4 and 9.5 respectively.

If one nitrite is released as a part of the primary electrode process as indicated by the data, the addition of ammonium ion in acidic solution might cause the nitrite ion to be removed by the following reaction:



If this reaction proceeded rapidly enough, it was proposed that the equilibrium concentration of NO_2^- at the electrode surface

TABLE 6

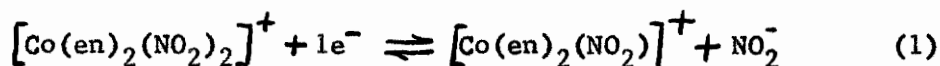
The Reduction of 0.001M $[\text{Co}(\text{en})_2(\text{NO}_2)_2]\text{NO}_3$ as a Function of Ammonium Ion Concentration in 0.2M Acetate Buffer at pH 5.1

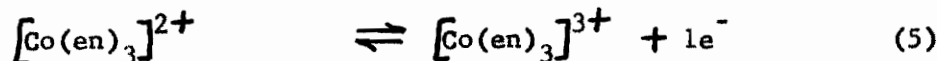
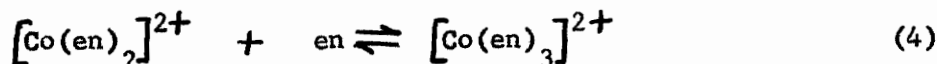
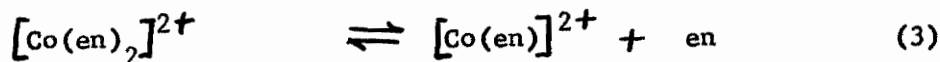
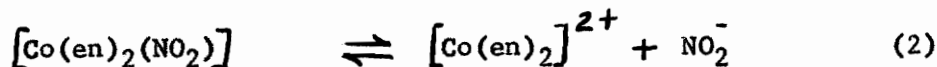
$[\text{NH}_4^+]$, M	$E_{1/2}$, volts	$i_1, \mu\text{a}$	Slope
0	-0.276	4.32	0.0579
0.040	-0.278	4.51	0.0570
0.200	-0.281	4.48	0.0577
0.400	-0.292	4.44	0.0561
0.500	-0.297	4.50	-
0.830	-0.309	4.46	0.0563
1.000	-0.312	4.37	0.0568
2.500	-0.330	4.30	0.0585

Note: KCl added to give ionic strength of 2.50M for all solutions.

could be reduced, thereby driving the electrode reaction to the right and shifting the $E_{1/2}$ to a more positive potential. As can be seen from Table 6, this is not the case and that in fact, the $E_{1/2}$ becomes more negative at high concentration of ammonium ion. The shift to more negative potentials is seen to be relatively small and may be due to the relatively massive concentration of ammonium ion inhibiting the diffusion of reacting species at the electrode surface, or interfering with electrode process in some other way. In any case, the nitrite-ammonium ion reaction appears to be too slow to have any detectable effect on the electrode reaction. On the basis of the data it appears that the first step of the reduction is a reversible electron transfer followed by a chemical reaction to produce other species. The fact that in solutions sufficiently acidic for virtually no cobalt (II) ethylenediamine complexes to exist only one wave results, suggests that at least one such complex is necessary to produce the double wave.

It may be noted that the $E_{1/2}$ of the second wave corresponds closely to the $E_{1/2}$ reported for $[\text{Co}(\text{en})_3]^{3+}$ by Laiten and Kivalo (32). If the second wave is due to $[\text{Co}(\text{en})_3]^{3+}$ it is possible to write the following reaction scheme:





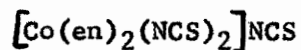
If all of the equilibria are rapid relative to the rate of diffusion, and if reaction 5 went to completion, two waves would result, the first corresponding to reaction 1 and the second corresponding to reaction 5. Both waves would have nearly equal wave heights, any differences being attributed to the difference in the size and shape of the electroactive species.

In the scheme presented here, the equilibria are assumed to be rapid, and in the potential region of the first limiting current, the oxidation of the $[\text{Co(en)}_3]^{2+}$ species is assumed to be complete. These assumptions imply that the net current of the second wave would be related to the equilibrium concentrations of $[\text{Co(en)}_2]^{2+}$ and ethylenediamine. Since both of these are dependent on pH, with increasing pH, more $[\text{Co(en)}_2]^{2+}$ and ethylenediamine are available for generation of $[\text{Co(en)}_3]^{2+}$ with the limiting concentration of $[\text{Co(en)}_3]^{2+}$ being equal to one-half of the total cobalt concentration.

The reversibility, nitrite ion dependence, and the pH independence of the first wave suggests that all reactions represented

by equations 1 to 5 are rapid, relative to the rate of diffusion. The height of the second wave being limited to approximately one-half of the total limiting current suggests that the reaction represented by equation 5 goes nearly to completion.

The results seem to be consistent with the following: rapid, reversible electron transfer; decomposition of the reduced species; and subsequent formation of tris-ethylenediamine cobalt (II); and oxidation of this species as it forms.



The half wave potentials and wave heights of the reduction waves are shown in Table 7 and Table 8, for electrolysis in phosphate and borate buffers, respectively, as a function of pH. The first wave in this case is sufficiently positive so that the mercury dissolution wave interferes with the first reduction wave. The mercury dissolution wave, which can be seen from the polarogram in Figure 7, causes difficulty in determining the exact zero current line and, therefore, the exact half wave potential of the first wave.

Figure 5 shows the relative height of the first reduction wave to the total limiting current as a function of hydroxide ion concentration.

Table 9 shows the dependence of the $E_{1/2}$ of the first wave on thiocyanate ion concentration. This dependence is shown

TABLE 7

The Reduction of 0.001M cis-[Co(en)₂(NCS)₂]NCS as a Function of pH in 0.2M Phosphate Buffer

pH	First Wave			Second Wave			Ir
	$E_{1/2}$, volts	$i_1, \mu a$	Slope	$E_{1/2}$, volts	$i_d, \mu a$ (total)	Slope	
7.13	-0.060	3.72	0.0810	-	-	-	-
7.35	-0.062	3.65	0.0790	-	-	-	-
7.78	-0.067	3.68	0.0781	-	-	-	-
8.34	-0.080	3.51	0.0925	-0.404	3.73	0.0690	0.941
9.15	-0.114	2.83	0.0815	-0.423	3.88	0.0675	0.729
10.23	-0.154	2.41	0.0995	-0.456	3.87	0.0720	0.623
11.60	-0.186	2.37	0.1275	-0.505	3.85	0.0680	0.616
12.31	-0.204	1.93	0.1025	-0.508	3.78	0.0805	0.515

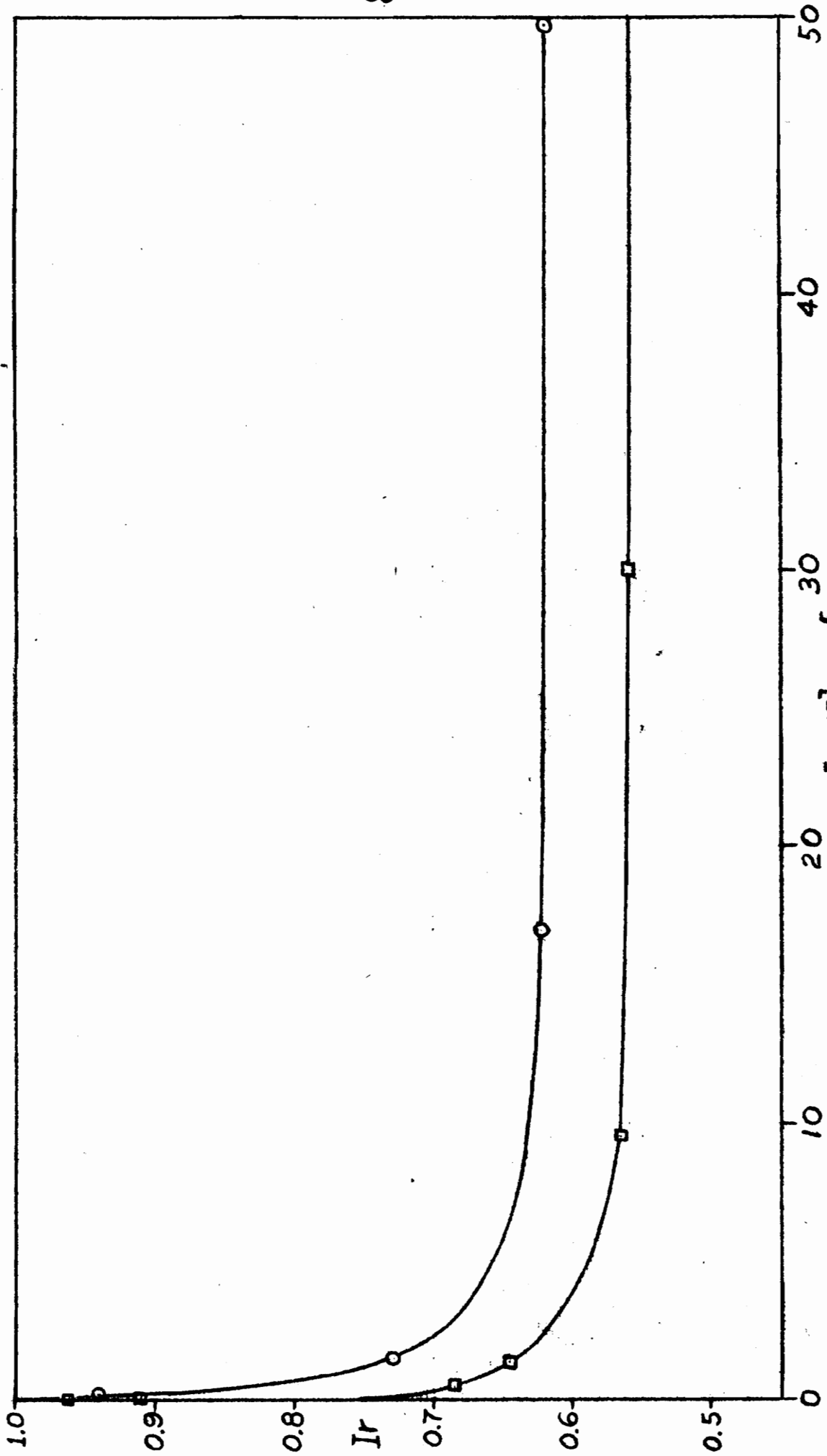
TABLE 8

The Reduction of 0.001M cis-[Co(en)₂(NCS)₂]NCS as a
Function of pH in 0.2M Borate Buffer

pH	First Wave			Second Wave			
	$E_{1/2}$, volts	$i_1, \mu\text{a}$	Slope	$E_{1/2}$, volts	$i_d, \mu\text{a}$ (total)	Slope	Ir
7.00	-0.074	4.28	0.0800	-0.330	4.45	-	0.963
7.08	-0.076	4.21	0.0845	-0.335	4.43	-	0.950
7.67	-0.086	3.96	0.0825	-0.341	4.35	-	0.910
8.70	-0.114	3.01	0.0880	-0.370	4.40	0.0640	0.681
9.13	-0.135	2.85	0.0825	-0.373	4.42	0.0630	0.645
9.98	-0.171	2.50	0.0910	-0.402	4.42	0.0708	0.566
11.53*	-0.217	1.58	0.1070	-0.413	4.42	0.0635	0.462

*Three waves developed at pH 11.53; the third wave showed $i_1 = 0.703$,
 $E_{1/2} = -0.633$, Slope = 0.0870.

Figure 5



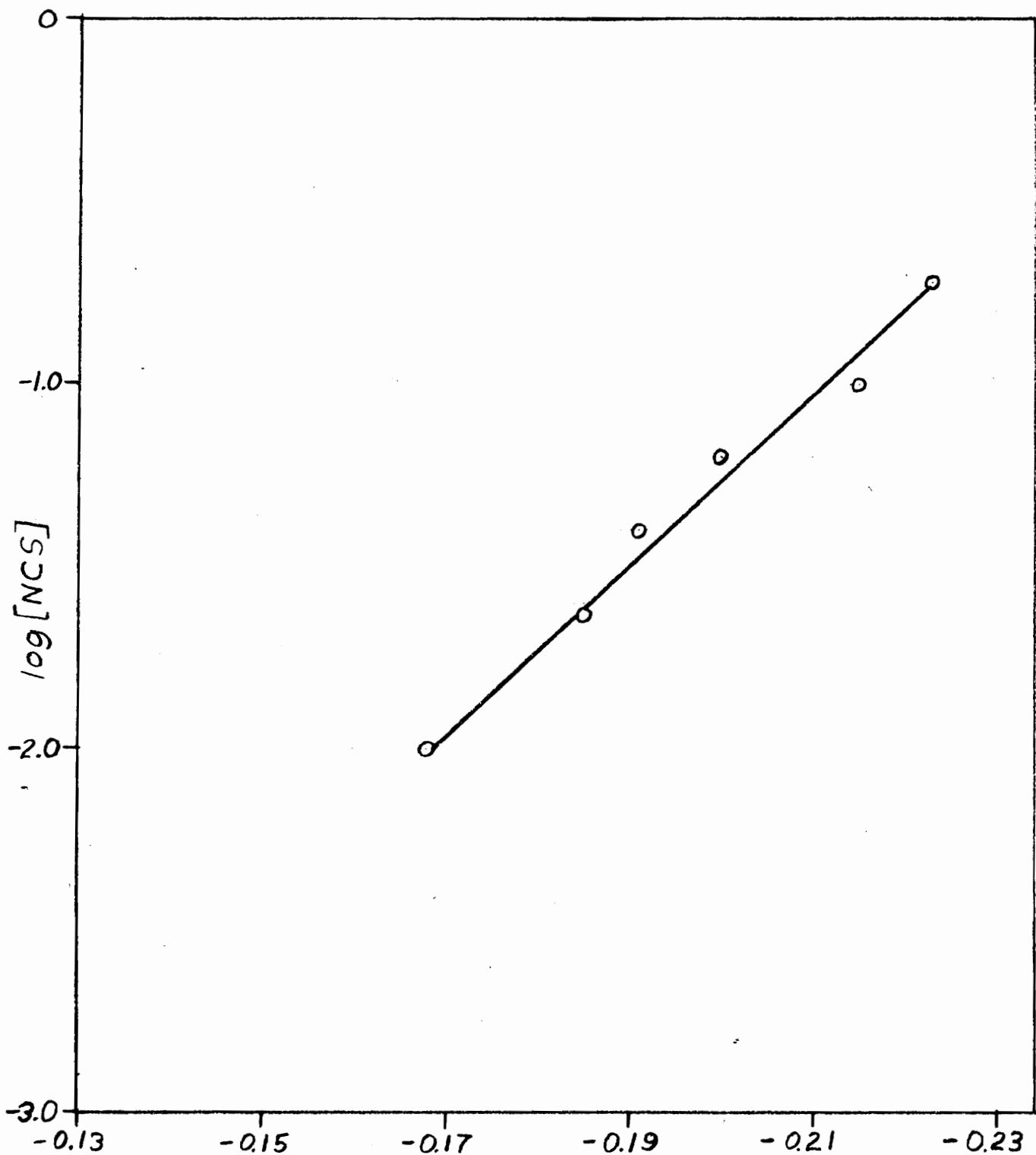
The Relative Height of First Reduction Wave of $[\text{Co}(\text{en})_2(\text{NCS})_2]\text{NCS}$ as a Function of $[\text{OH}^-]$. \circ , Phosphate Buffer; \square , Borate Buffer.

TABLE 9

The Reduction of 0.001M cis-[Co(en)₂(NCS)₂]NCS as a Function of Thiocyanate Ion Concentration in 0.2M Phosphate Buffer at pH 10.0

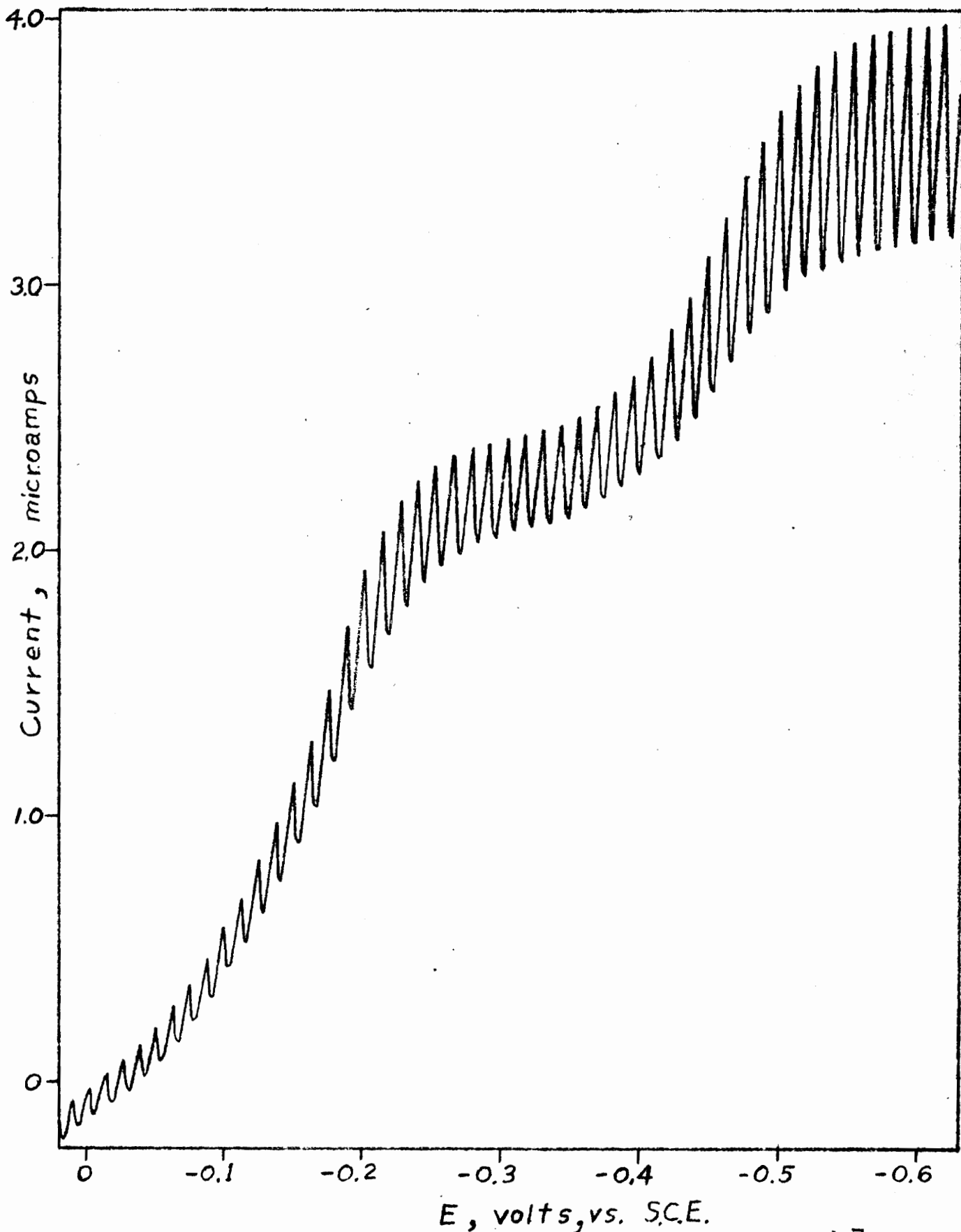
$[\text{NCS}^-]$, M	First Wave			Second Wave			Ir
	$E_{1/2}$, volts	$i_1, \mu\text{a}$	Slope	$E_{1/2}$, volts	$i_d, \mu\text{a}$ (total)	Slope	
0	-0.132	2.18	0.0940	-0.450	3.81	0.0715	0.573
0.010	-0.168	1.88	0.0680	-0.445	3.76	0.0710	0.500
0.020	-0.185	1.72	0.0692	-0.439	3.64	0.0760	0.472
0.040	-0.193	1.73	0.0705	-0.440	3.75	0.0770	0.462
0.070	-0.202	1.68	0.0655	-0.435	3.71	0.0775	0.453
0.100	-0.215	1.65	0.0675	-0.436	3.65	0.0760	0.465
0.144	-0.223	1.72	0.0665	-0.435	3.69	0.0750	0.465

Figure 6



The Half Wave Potential of the First Reduction Wave of $[Co(en)_2(NCS)_2]NCS$ as a Function of Thiocyanate Ion Concentration in Phosphate Buffer

-36-
Figure 7

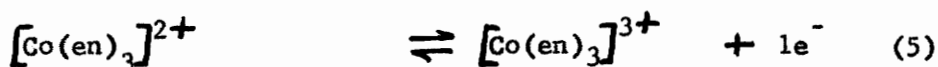
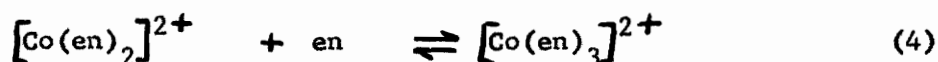
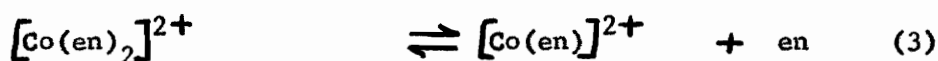
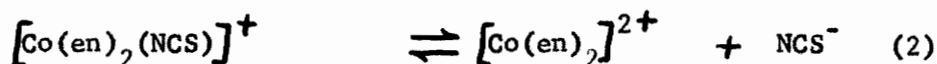
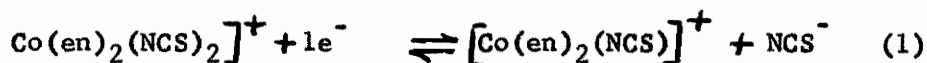


Polarogram of the Reduction of $[\text{Co}(\text{en})_2(\text{NCS})_2]\text{NCS}$
in Phosphate Buffer at pH 10.23

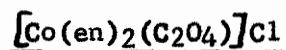
graphically in Figure 6. The magnitude of the shift in $E_{1/2}$ is of the order of 0.045 volts per ten-fold change in thiocyanate ion concentration. This fact is in accordance with observation that the first wave is irreversible.

An attempt was made to reduce the mercury-thiocyanate anodic interference by converting the compound from a thiocyanate salt to a nitrate salt. A solution of the compound was passed through an anion exchange column which had been previously charged with nitrate ion. The resulting nitrate salt was then electrolyzed in the same buffer solution as previously used. No reduction in the interference from the mercury reaction could be detected. The $E_{1/2}$ and wave heights of both waves were identical to those of the thiocyanate salt

The $E_{1/2}$ of the second wave, and the relative height of the second wave with respect to pH appear to be due to $[\text{Co}(\text{en})_3]^{2+}$ as in the case of the $[\text{Co}(\text{en})_2(\text{NO}_2)_2]\text{NO}_3$. If this is the case, the following reaction scheme may be written.



The equilibria in this case appear to be not too rapid, relative to the rate of diffusion as indicated by the irreversibility of the first wave. The reaction represented by equation 5 does not appear to go nearly to completion, as indicated by the relative height of the second wave in the limiting case of high pH. Any conclusion as to the mechanism of the electrode reaction has to be viewed in the light of the interference of the mercury dissolution wave on the first reduction wave, the irreversibility and apparent slight pH dependence of the first wave.



The half wave potentials and wave heights for the reduction of oxalato-bis-(ethylenediamine) cobalt (III) chloride as a function of pH are given in Tables 10 and 11, for reductions in phosphate and in borate buffers, respectively. The half wave potential of the first wave was in agreement with the results obtained by Tsuchida (2).

Solutions were also prepared in which 0.1M oxalate ion was added. No detectable shift in the $E_{1/2}$ of the first wave was apparent and no changes were evident in the shape of the wave.

On the assumption that oxalate ion is released as a part of the primary electrode process, the presence of calcium ion in the solution might cause the equilibrium of the electrode reaction

TABLE 10

The Reduction of 0.001M $[\text{Co(en)}_2(\text{C}_2\text{O}_4)]\text{Cl}$ as a Function
of pH in 0.2M Phosphate Buffer

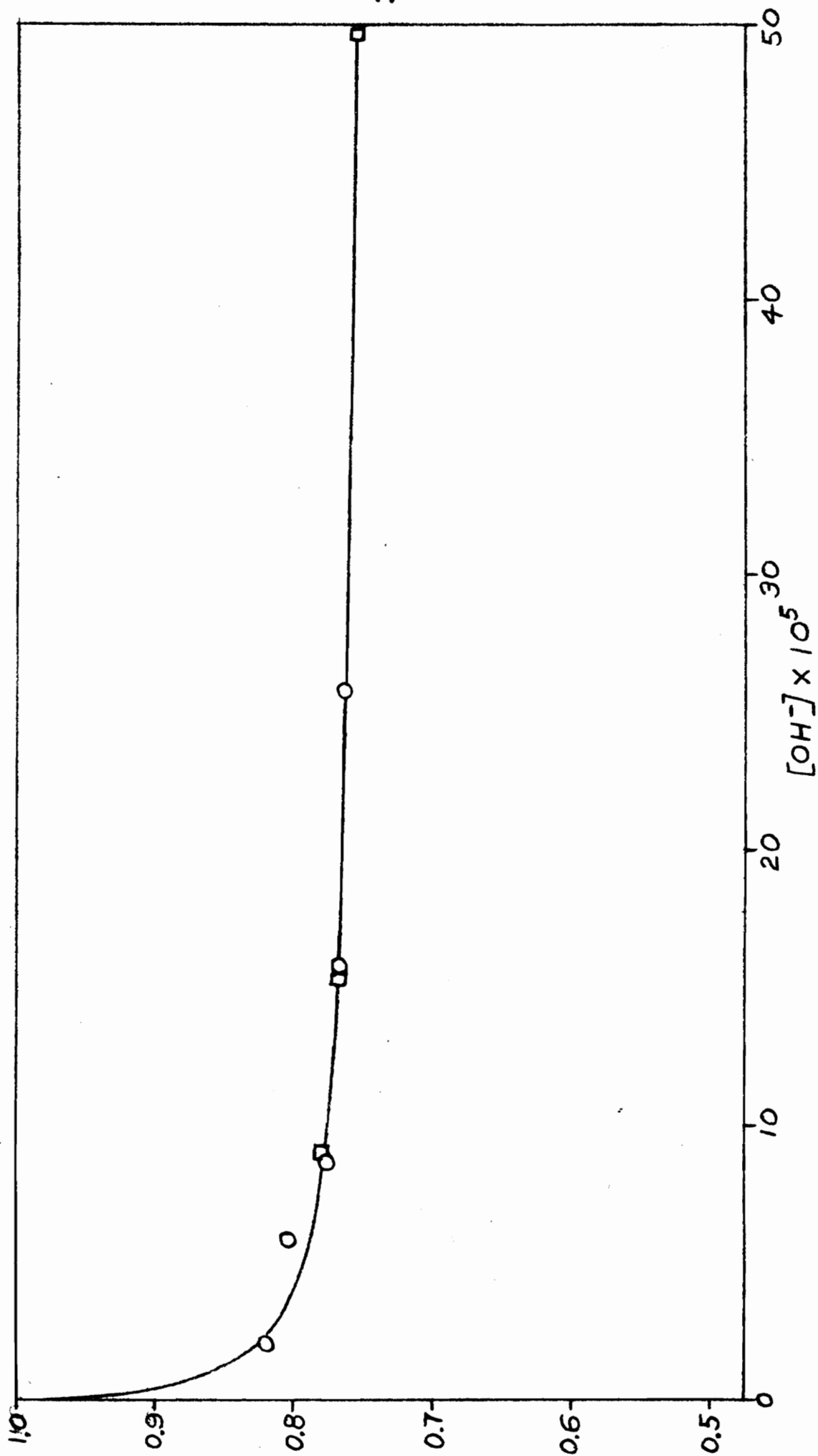
pH	First Wave			Second Wave			
	$E_{1/2}$, volts	$i_1, \mu\text{a}$	Slope	$E_{1/2}$, volts	$i_d, \mu\text{a}$ (total)	Slope	Ir
5.73	-0.315	3.24	0.0815	-	-	-	-
5.77	-0.316	3.25	0.0795	-	-	-	-
5.85	-0.315	3.25	0.0760	-	-	-	-
6.22	-0.316	3.29	0.0730	-	-	-	-
6.67	-0.316	3.24	0.0960	-	-	-	-
7.08	-0.317	3.20	0.0815	-	-	-	-
7.70	-0.317	3.28	0.0810	-	-	-	-
9.94	-0.316	2.54	0.0870	-0.472	3.27	0.0550	0.779
10.20	-0.316	2.53	0.0865	-0.492	3.31	0.0565	0.765
10.86	-0.314	2.48	0.0850	-0.502	3.25	0.0555	0.762
10.93	-0.315	2.45	0.0863	-0.496	3.28	0.0560	0.746
11.21	-0.318	2.47	0.0845	-0.522	3.28	0.0585	0.753
11.50	-0.317	2.38	0.0851	-0.515	3.29	0.0595	0.724
11.60	-0.314	2.40	0.0860	-0.530	3.25	0.0590	0.738
11.86	-0.318	2.33	0.0745	-0.520	3.28	0.0550	0.711
12.18	-0.316	2.31	0.0785	-0.519	3.30	0.0595	0.700

TABLE 11

The Reduction of 0.001M $[\text{Co(en)}_2(\text{C}_2\text{O}_4)]\text{Cl}$ as a Function
of pH in 0.2M Borate Buffer

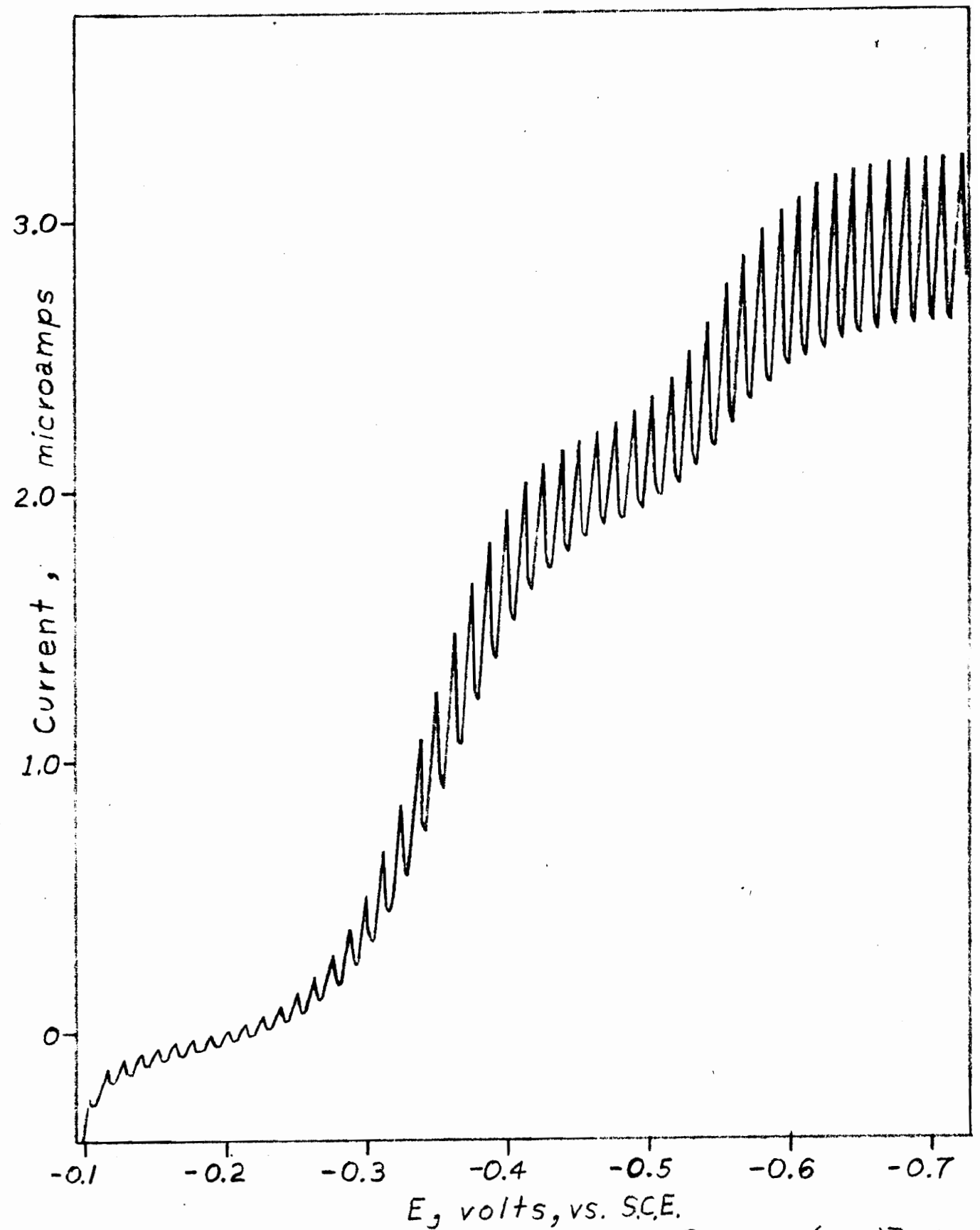
pH	First Wave			Second Wave			
	$E_{1/2}$, volts	$i_1, \mu\text{a}$	Slope	$E_{1/2}$ volts	$i_d, \mu\text{a}$ (total)	Slope	Ir
6.38	-0.288	3.78	0.0805	-	-	-	-
6.70	-0.288	3.73	0.0750	-	-	-	-
7.41	-0.290	3.76	0.0755	-	-	-	-
8.10	-0.294	3.81	0.0825	-	-	-	-
8.57	-0.296	3.80	0.0881	-	-	-	-
8.73	-0.303	3.81	0.0835	-	-	-	-
9.29	-0.297	3.55	0.0810	-0.429	3.75	0.0553	0.820
9.78	-0.303	3.02	0.0810	-0.439	3.75	0.0575	0.806
9.94	-0.301	2.92	0.0825	-0.447	3.73	0.0550	0.781
10.20	-0.298	2.88	0.0831	-0.440	3.75	0.0565	0.768
10.41	-0.312	2.85	0.0835	-0.447	3.73	0.0545	0.765
11.27	-0.302	2.38	0.0832	-0.453	3.78	0.0580	0.627
11.45	-0.320	2.37	0.0975	-0.452	3.75	0.0535	0.631
12.50	-0.317	3.80	0.1050	-	-	-	1.000

Figure 8



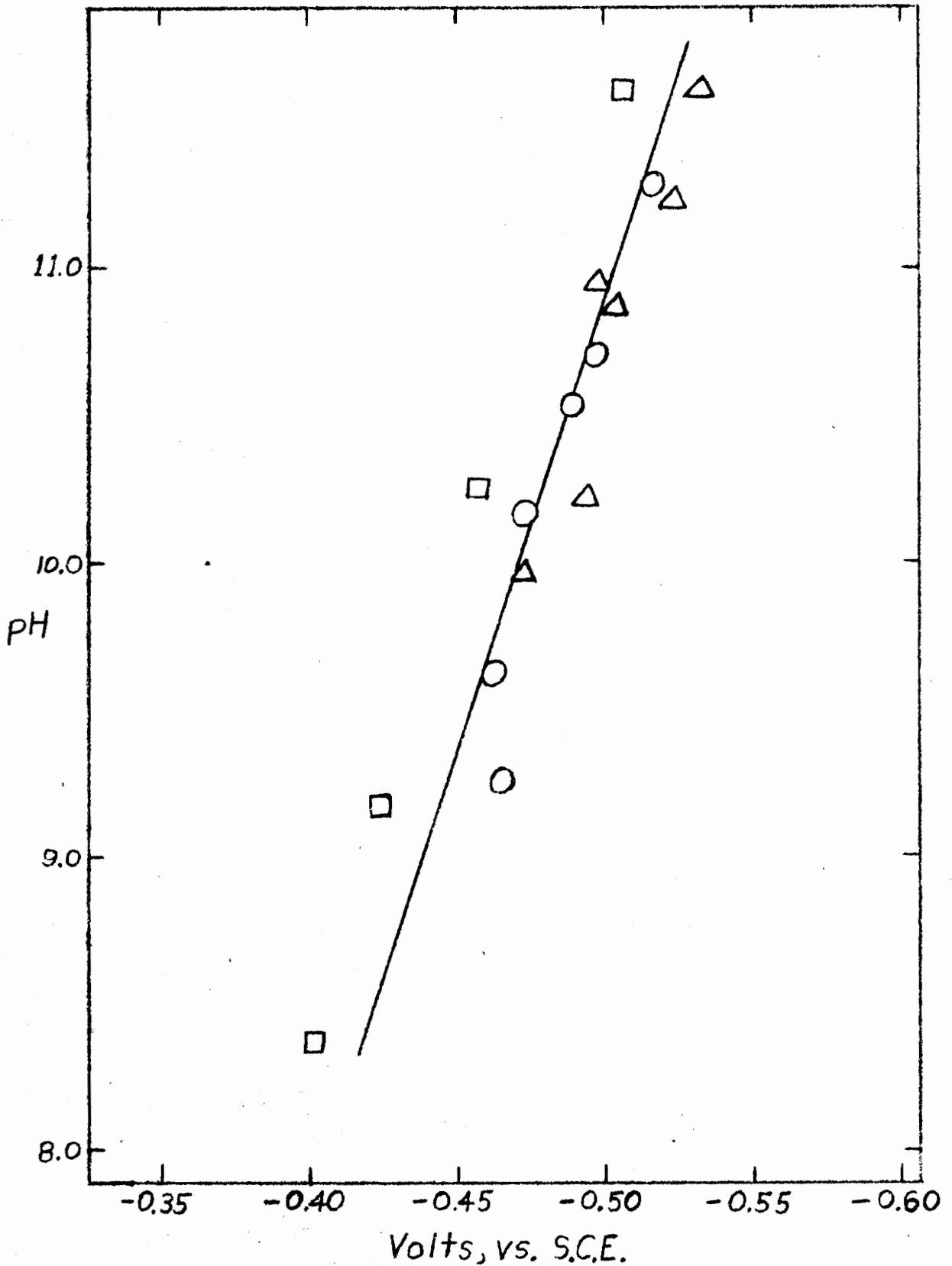
The Relative Height of the First Reduction Wave of $[Co(en)_2(C_2O_4)]Cl$ as a Function of Hydroxide Ion Concentration; in Phosphate: ○, in Borate: □

-42-
Figure 9



Polarogram of the Reduction of $[\text{Co}(\text{en})_2(\text{C}_2\text{O}_4)]\text{Cl}$
in Phosphate Buffer at pH 12.18

Figure 10

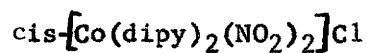


The Half Wave Potential versus pH for the Ethylenediamine Complexes: $[\text{Co}(\text{en})_2(\text{NO}_2)_2]\text{NO}_3$, ○; $[\text{Co}(\text{en})_2(\text{NCS})_2]\text{NCS}$, ◻; $[\text{Co}(\text{en})_2(\text{C}_2\text{O}_4)]\text{Cl}$, Δ.

to be shifted, thereby shifting the $E_{1/2}$ of the first wave. The failure of calcium ion to cause any detectable shift in the $E_{1/2}$ indicates further that the reduction product is not participating in a reversible electrode reaction involving oxalate ion.

Figure 8 shows the relative height of the first wave to the total limiting current as a function of hydroxide ion concentration. Figure 9 shows a representative polarogram in phosphate buffer.

The slight pH dependance of the first wave is in line with the irreversibility of the wave. The relative height of the second wave in the limiting case of high pH being somewhat less than one-half of the total limiting current may be accounted for by a relatively slower decomposition of the product of the primary electrode process. The second wave in this case again appears to be due to oxidation of $[\text{Co}(\text{en})_3]^{2+}$ as in the case of the dinitro and the dithiocyanato compounds. Figure 10 shows a comparison of the $E_{1/2}$ of the second wave as a function of pH for all three of the bis-ethylenediamine complexes.



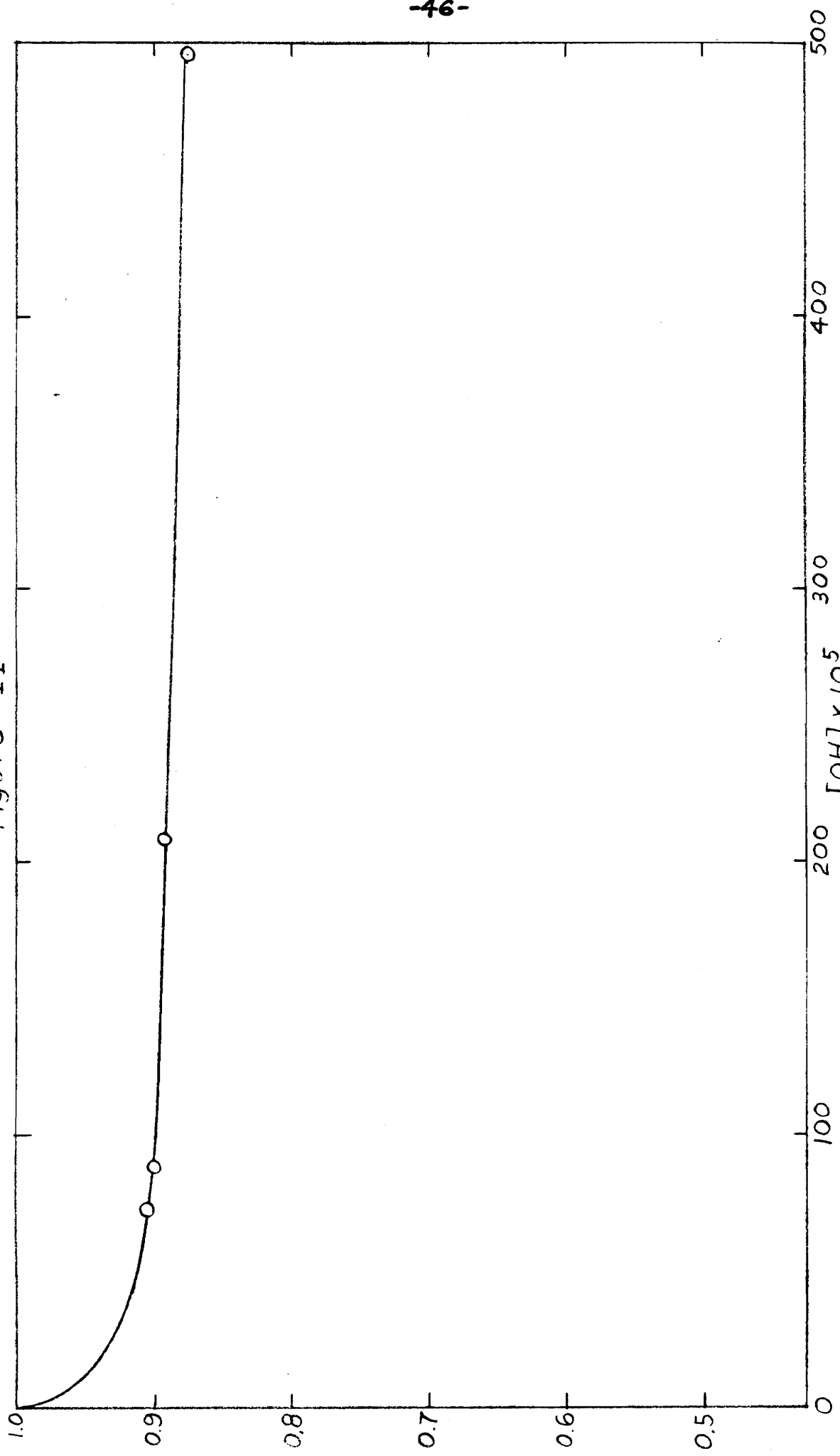
The data from the reductions in phosphate buffer are given in Table 12. Figure 11 shows the height of the first wave, relative to the total limiting current, as a function of hydroxide ion concentration.

TABLE 12

The reduction of 0.001M $[\text{Co}(\text{dipy})_2(\text{NO}_2)_2]\text{Cl}$ as a Function of pH in 0.2M Phosphate Buffer

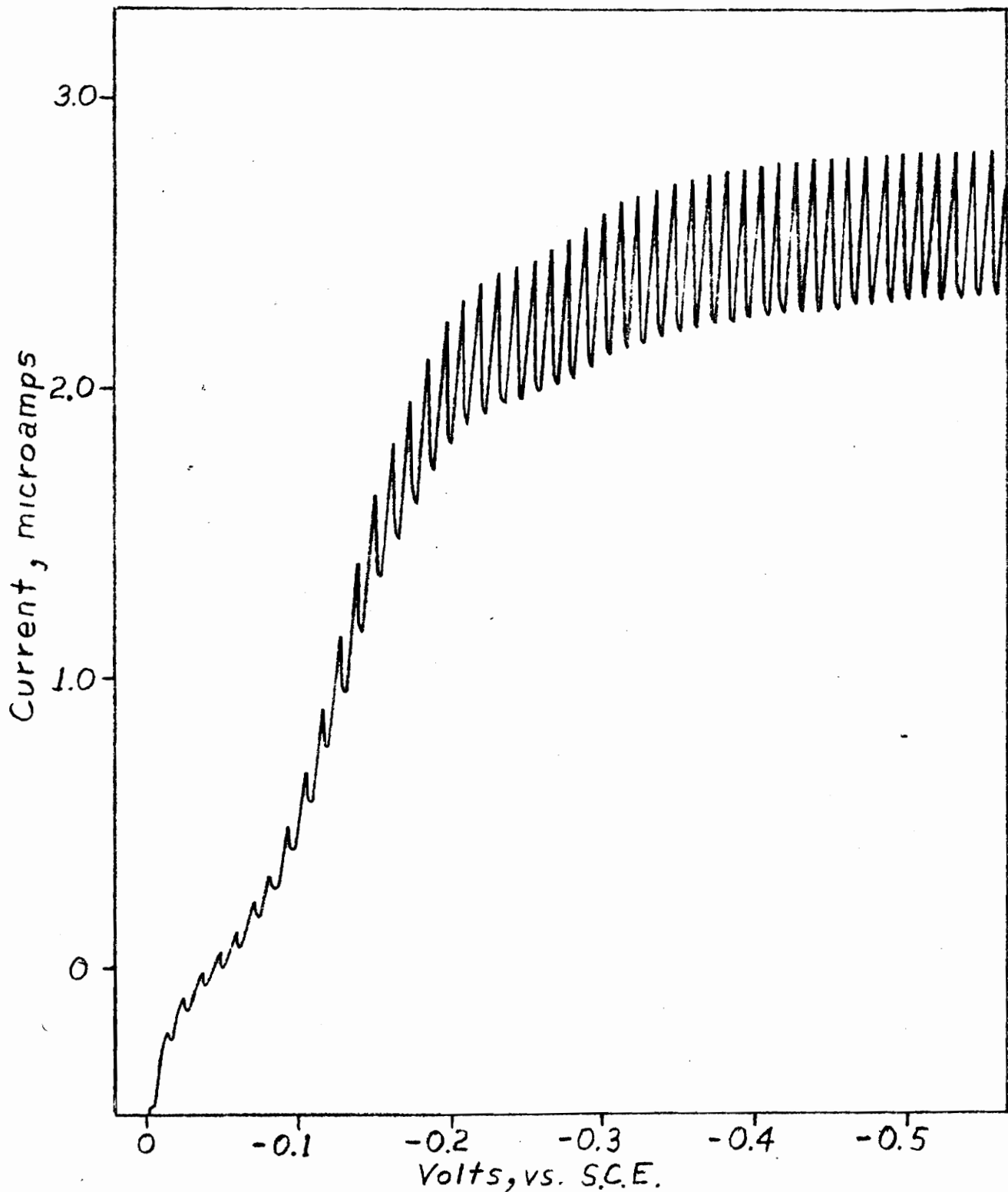
pH	First Wave			Second Wave			
	$E_{1/2}$, volts	$i_l, \mu\text{a}$	Slope	$E_{1/2}$, volts	$i_d, \mu\text{a}$ (total)	Slope	Ir
4.33	0.086	2.86	0.0890	-	-	-	-
6.67	0.109	2.81	0.0995	-	-	-	-
8.63	-0.004	2.85	0.0650	-	-	-	-
9.27	-0.002	2.83	0.0640	-	-	-	-
10.86	-0.072	2.63	0.0645	-0.210	2.90	0.0575	0.906
10.95	-0.106	2.55	0.0615	-0.245	2.83	0.0585	0.900
11.32	-0.132	2.58	0.0600	-0.303	2.89	0.0595	0.893
12.37	-0.240	2.57	0.0750	-0.376	2.86	0.0590	0.797

Figure 11



The Relative Height of the First Reduction Wave of $[\text{Co}(\text{dipy})_2(\text{NO}_2)_2]\text{Cl}$ as a Function of Hydroxide Ion Concentration in Phosphate Buffer.

Figure 12

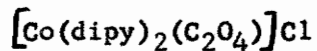


Polarogram of the Reduction of $[\text{Co}(\text{dipy})_2(\text{NO}_2)_2]\text{Cl}$ in Phosphate Buffer at pH 11.32

The first wave developed at so positive a potential that the mercury oxidation wave interfered with development of the wave. An example of the reduction waves may be seen in Figure 12.

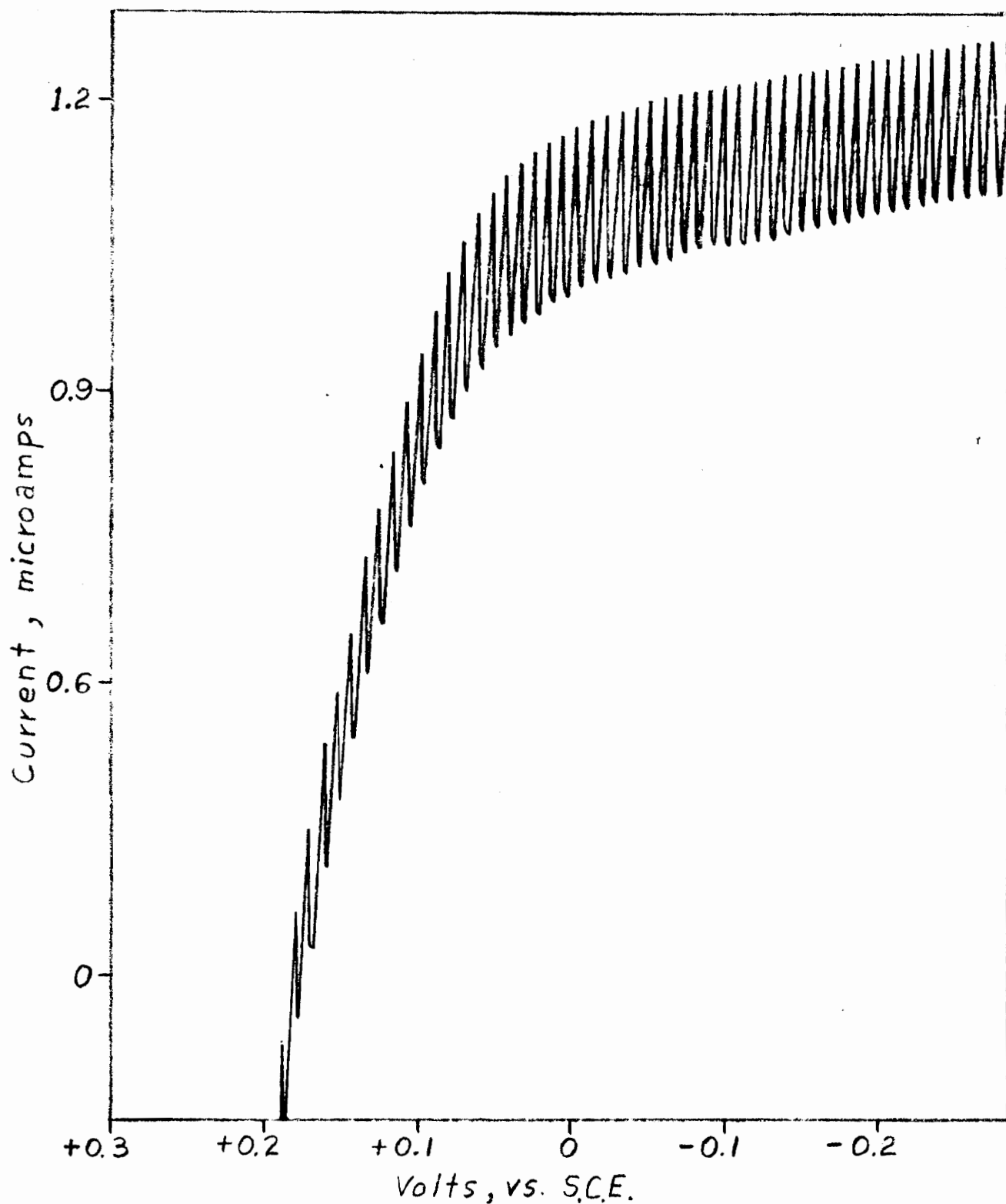
The addition of nitrite ion appears to have no effect on the $E_{1/2}$ of the first wave. The apparent shift in the $E_{1/2}$ with pH may be real, or it may be due to the mercury anodic wave, which also shifts to more negative potentials with increased pH.

It may be noted that the height of the second wave, relative to the total limiting current, is approximately one-third the height of the second wave of the ethylenediamine complexes at the same pH level. This, along with the fact that the $E_{1/2}$ of the second wave is approximately 0.13 volts more negative than the $E_{1/2}$ of the first wave suggest that a mechanism similar to that of the ethylenediamine complexes may be involved here also. The dipyridyl case seems to be more complicated though. It is noted that the slope of the first wave is quite irreversible in acidic or neutral solutions but seems to become reversible, or nearly so in highly alkaline solutions. Also the $E_{1/2}$ of the second wave appears to be much more sensitive to changes in pH than does the ethylenediamine complex.



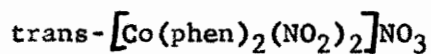
The reduction wave, as seen in Figure 13, is completely masked by the mercury anodic wave. Attempts were made to obtain polarograms

-49-
Figure 13

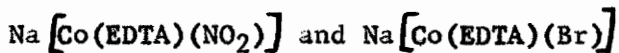


Polarogram of the Reduction of $[\text{Co}(\text{dipy})_2(\text{C}_2\text{O}_4)]\text{Cl}$
in Phosphate Buffer at pH 5.90

in highly acidic buffers to shift the mercury wave to a positive enough potential so as to give a sufficiently developed cathodic wave for interpretation. It was found that the $E_{1/2}$ is more positive than $+0.20$ volts versus the S.C.E. and that no interpretation of the wave can be made.



The half wave potential of the dinitro-bis-(phenanthroline) complex was also too positive to measure due to the mercury anodic wave. An additional problem is involved with this complex in that in mildly alkaline solutions aquation occurs, with a corresponding decrease in the total limiting current of the wave.

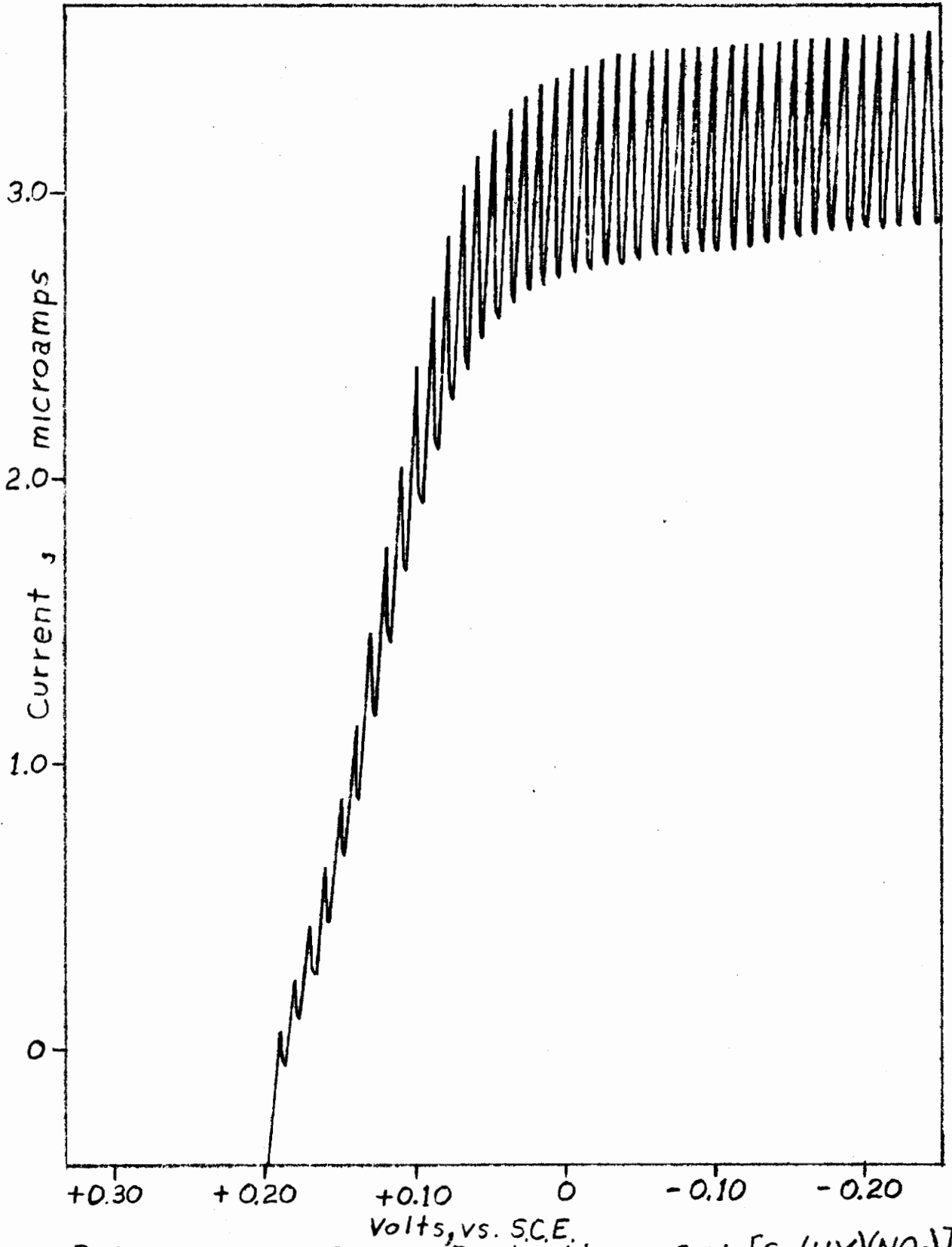


Both of these complexes show half wave potentials more positive than $+0.20$ volts versus the S.C.E. and both are susceptible to aquation. The bromo complex, even in acidic solution will turn from a green-blue to a red color in 15 to 20 minutes. The aquation of the nitro complex is harder to distinguish but is noticeably advanced within an hour in neutral solution.

Results Obtained Using the Rotating Platinum Electrode

For all three of the ethylenediamine complexes, the $E_{1/2}$ of the waves and limiting current were not reproducible. The results

Figure 14



Polarogram of the Reduction of $\text{Na}[\text{Co}(\text{HY})(\text{NO}_2)]$ in Phosphate Buffer at pH 6.10

for trans- $[\text{Co}(\text{en})_2(\text{NO}_2)_2]\text{NO}_3$ are given in Table 13, for cis- $[\text{Co}(\text{en})_2(\text{NCS})_2]\text{NCS}$ in Table 14, and for $[\text{Co}(\text{en})_2(\text{C}_2\text{O}_4)]\text{Cl}$ in Table 15. There does appear to be no detectable pH effect on the reduction of any of the three complexes. All three complexes show irreversible behavior at the rotating platinum electrode. Ligand variations were conducted on all three complexes with no observable effect on the $E_{1/2}$ of the wave. Representative polarograms for trans- $[\text{Co}(\text{en})_2(\text{NO}_2)_2]\text{NO}_3$, cis- $[\text{Co}(\text{en})_2(\text{NCS})_2]\text{NCS}$ and $[\text{Co}(\text{en})_2(\text{C}_2\text{O}_4)]\text{Cl}$ are shown in Figures 15, 16, and 17 respectively. The oxalato complex showed less variation in wave height and in $E_{1/2}$ than the other two ethylenediamine complexes but this was still several times the error inherent in the measurements.

For the reduction of cis- $[\text{Co}(\text{dipy})_2(\text{NO}_2)_2]\text{Cl}$ at the platinum electrode, the variability in $E_{1/2}$ is much less than for the ethylenediamine complexes. This variation in $E_{1/2}$ is only a little more than the sensitivity of the instrument itself. The wave height appears to vary more than should be expected. The wave was well developed, as can be seen from the polarogram in Figure 18. The data for the reduction in phosphate buffer are given in Table 16 and for acetate buffer in Table 17. The waves were all irreversible in phosphate as well as in acetate buffer.

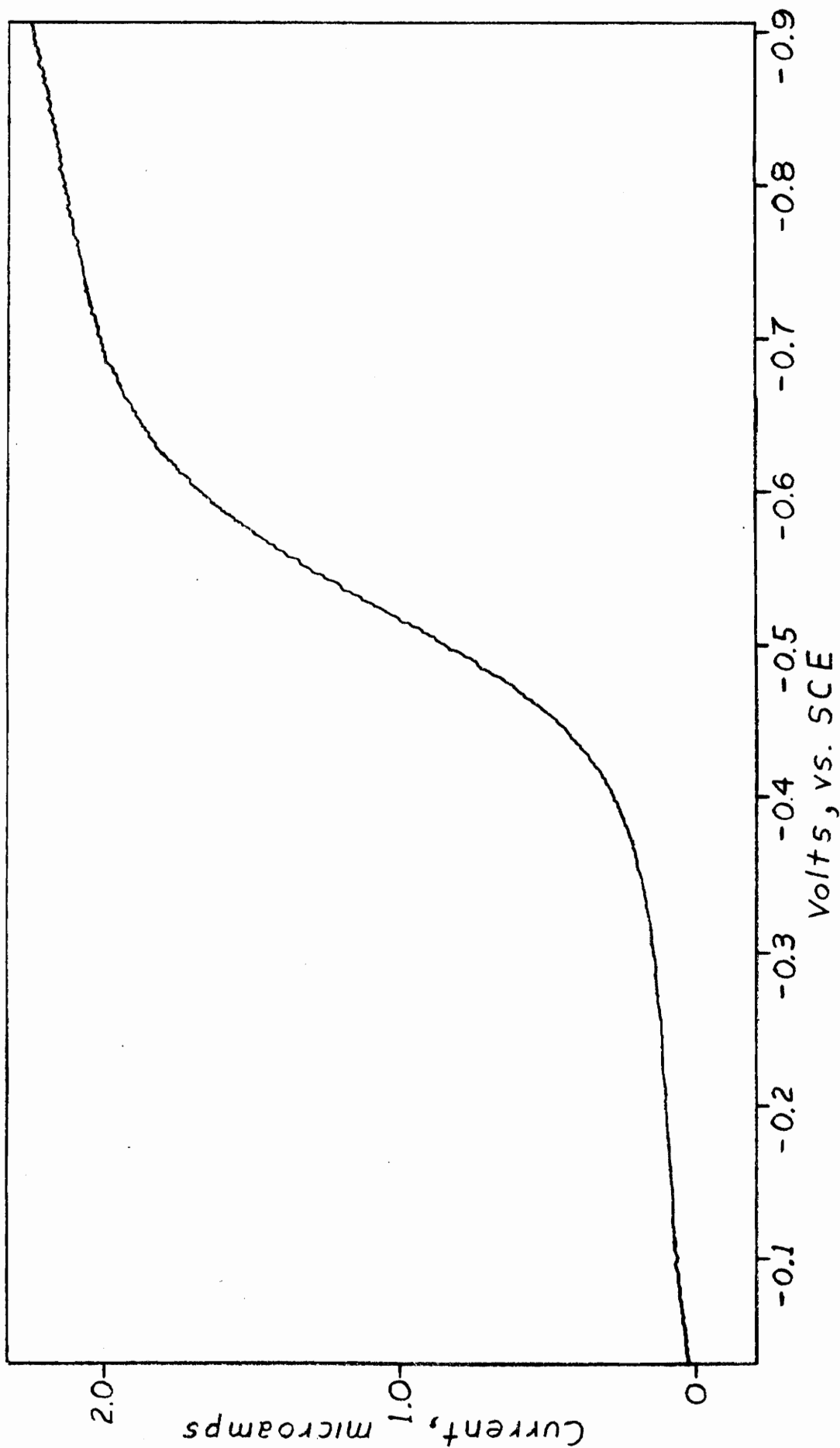
The reduction wave for $[\text{Co}(\text{dipy})_2(\text{C}_2\text{O}_4)]\text{Cl}$ was not as well developed as the dinitro complex. The variations in $E_{1/2}$ and wave

TABLE 13

The Reduction of 0.001M $[\text{Co}(\text{en})_2(\text{NO}_2)_2]\text{NO}_3$ as a Function of pH in 0.5M Phosphate Buffer at the Rotating Platinum Electrode

<u>pH</u>	<u>$E_{1/2}$, volts</u>	<u>$i_l, \mu\text{a}$</u>	<u>Slope</u>
6.95	-0.604	4.62	0.0910
7.85	-0.556	3.54	0.1165
10.06	-0.590	5.50	0.1538
10.61	-0.510	1.90	0.1377
10.65	-0.470	2.85	0.1275
10.67	-0.527	1.78	0.1114

Figure 15



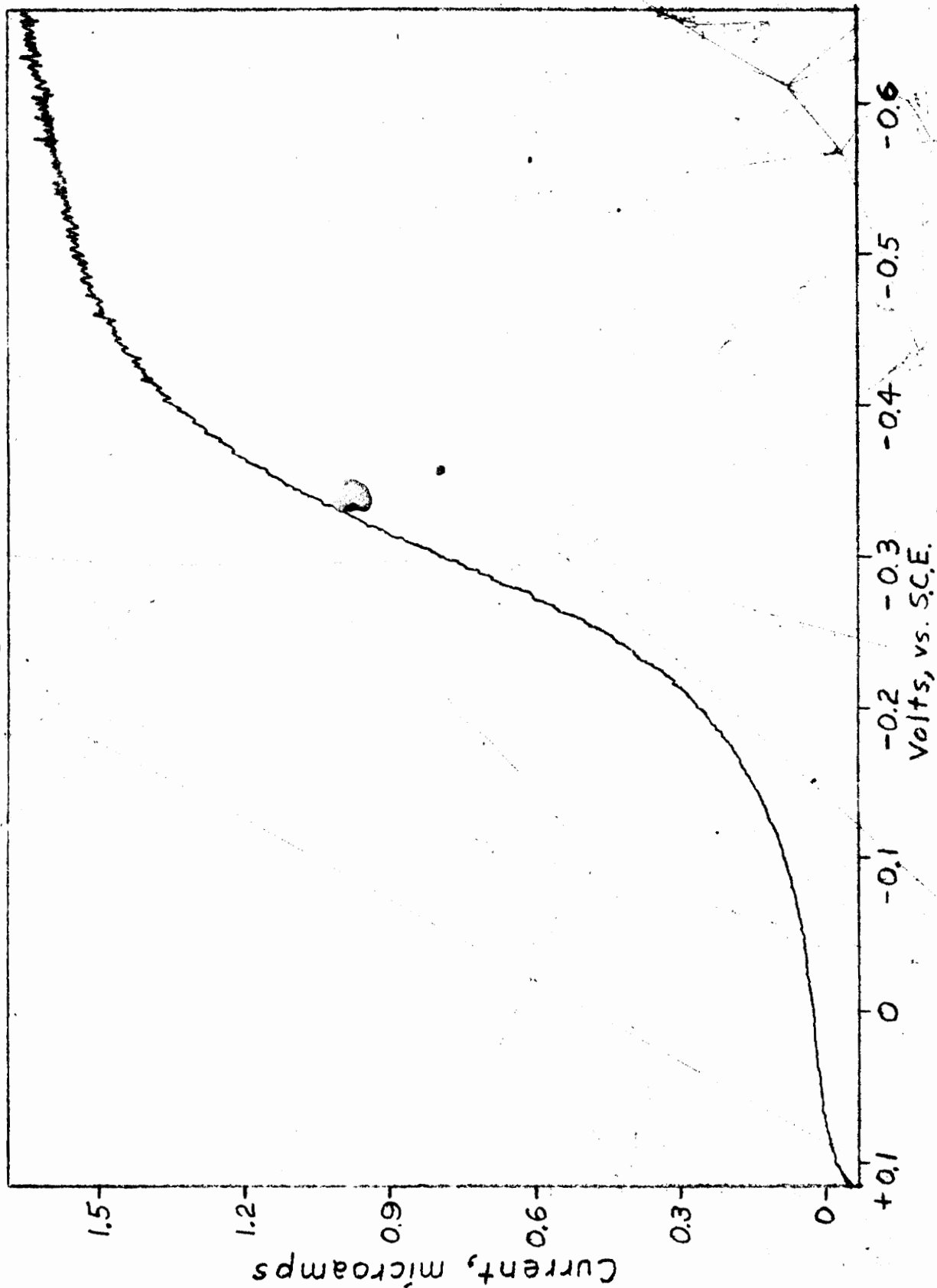
Polarogram of the Reduction of $[\text{Co}(\text{en})_2(\text{NO}_2)_2]\text{NO}_3$, at the Rotating Platinum Electrode, in Phosphate Buffer at pH 10.67

TABLE 14

The Reduction of 0.005M $[\text{Co}(\text{en})_2(\text{NCS})_2]\text{NCS}$ as a Function of pH in 0.5M Phosphate Buffer at the Rotating Platinum Electrode

<u>pH</u>	<u>$E_{1/2}$, volts</u>	<u>$i_1, \mu\text{a}$</u>	<u>Slope</u>
5.90	-0.328	2.31	0.1320
6.62	-0.344	3.02	0.1315
7.30	-0.265	3.53	0.1275
9.21	-0.236	4.06	0.0975
10.00	-0.280	2.56	0.0753
10.23	-0.307	2.54	0.1325
10.87	-0.303	3.58	0.0870
11.08	-0.422	3.47	0.1675
11.20	-0.420	3.05	0.1205
11.30	-0.251	3.82	0.0930
11.65	-0.274	4.05	0.0995

Figure 16



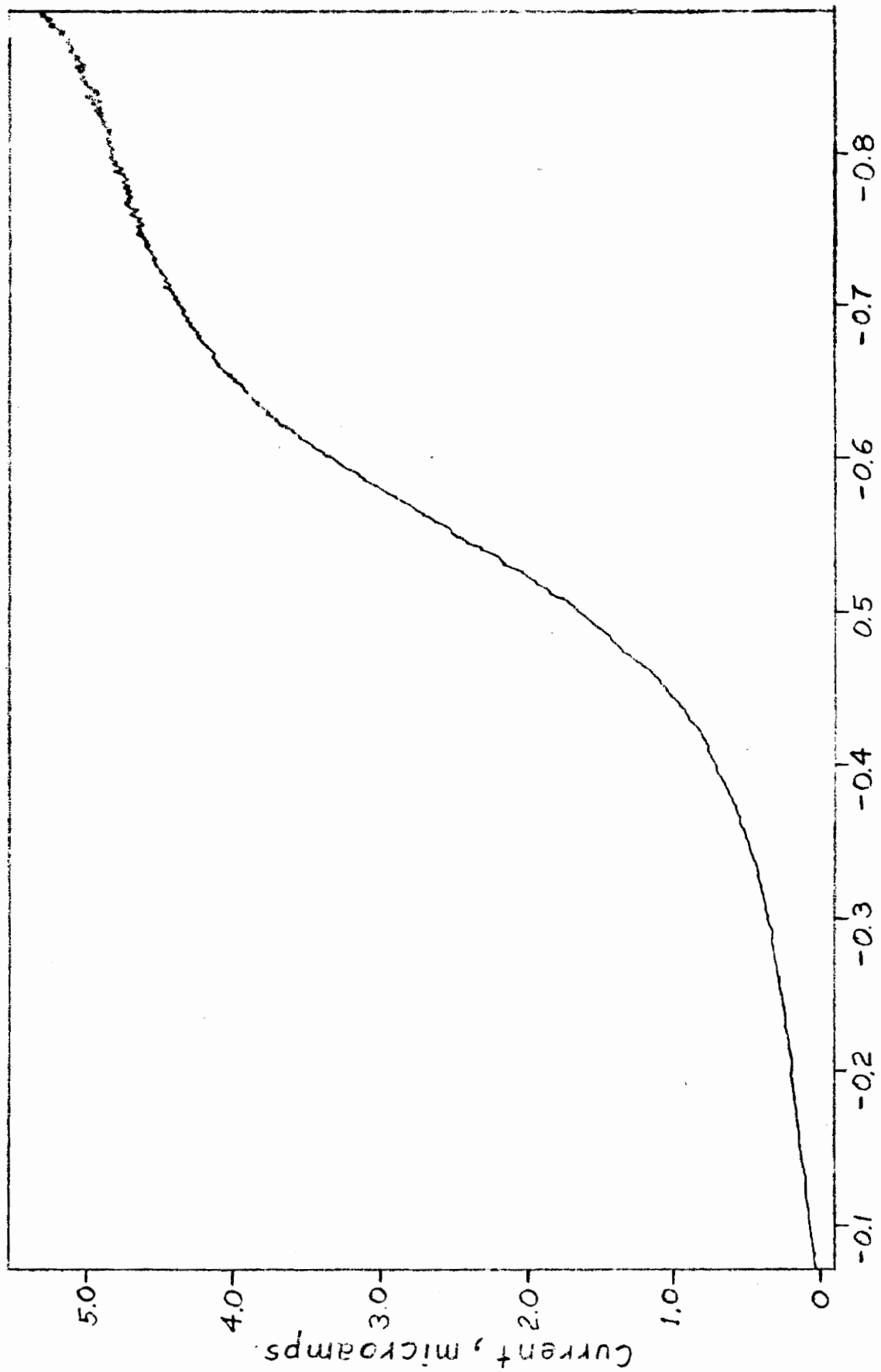
Polarogram of the Reduction of $[\text{Co}(\text{en})_2(\text{NCS})_2]\text{NCS}$, at the Rotating Platinum Electrode, in Phosphate Buffer at pH 9.25

TABLE 15

The Reduction of 0.001M $[\text{Co}(\text{en})_2(\text{C}_2\text{O}_4)]\text{Cl}$ as a Function of pH in 0.5M Phosphate Buffer at the Rotating Platinum Electrode

<u>pH</u>	<u>$E_{1/2}$, volts</u>	<u>$i_1, \mu\text{a}$</u>	<u>Slope</u>
9.31	-0.546	3.77	0.1753
9.93	-0.526	3.80	0.1383
10.05	-0.506	3.24	0.1255
10.51	-0.562	3.92	0.1460
11.20	-0.548	4.23	0.1442
11.23	-0.527	4.10	0.1275
11.34	-0.515	3.98	0.1295
11.56	-0.551	3.78	0.1290

Figure 17



Polarogram of the Reduction of $[\text{Co}(\text{en})_2(\text{C}_2\text{O}_4)]\text{Cl}$ at the Rotating Platinum Electrode in Phosphate Buffer at pH 11.56

height were greater than those observed for the dinitro complex. The wave was irreversible and the diffusion current region was not as well defined as for the dinitro complex, as can be seen from Figure 19. No shift in the wave was observed in the presence of oxalate ion. Table 18 gives the data for the reduction in phosphate buffers and Table 19 gives the data for acetate buffers.

The reduction of $\text{trans-}[\text{Co}(\text{phen})_2(\text{NO}_2)_2]\text{NO}_3$ at the platinum electrode in phosphate and acetate buffers, as shown in Tables 20 and 21, respectively, gave a half wave potential which varied over a range of 0.047 volts and which was approximately 0.07 volts more positive than for $\text{cis-}[\text{Co}(\text{dipy})_2(\text{NO}_2)_2]\text{NO}_3$. The waves showed a well developed limiting current region. A wider variation in the wave height was observed in phosphate buffer than in acetate. An example of the polarograms obtained is shown in Figure 20. All waves were irreversible.

Neither of the ethylenediamine tetraacetate complexes gave well developed waves at the platinum electrode. This may be accounted for by the rapid aquation of these complexes or by some factor which prevents them from being reduced at the platinum surface.

A comparison of the half wave potentials obtained at the dropping mercury electrode and at the rotating platinum electrode

TABLE 16

The Reduction of 0.0005M $[\text{Co}(\text{dipy})_2(\text{NO}_2)_2]\text{Cl}$ as a Function of pH in 0.5M Phosphate Buffer at the Rotating Platinum Electrode

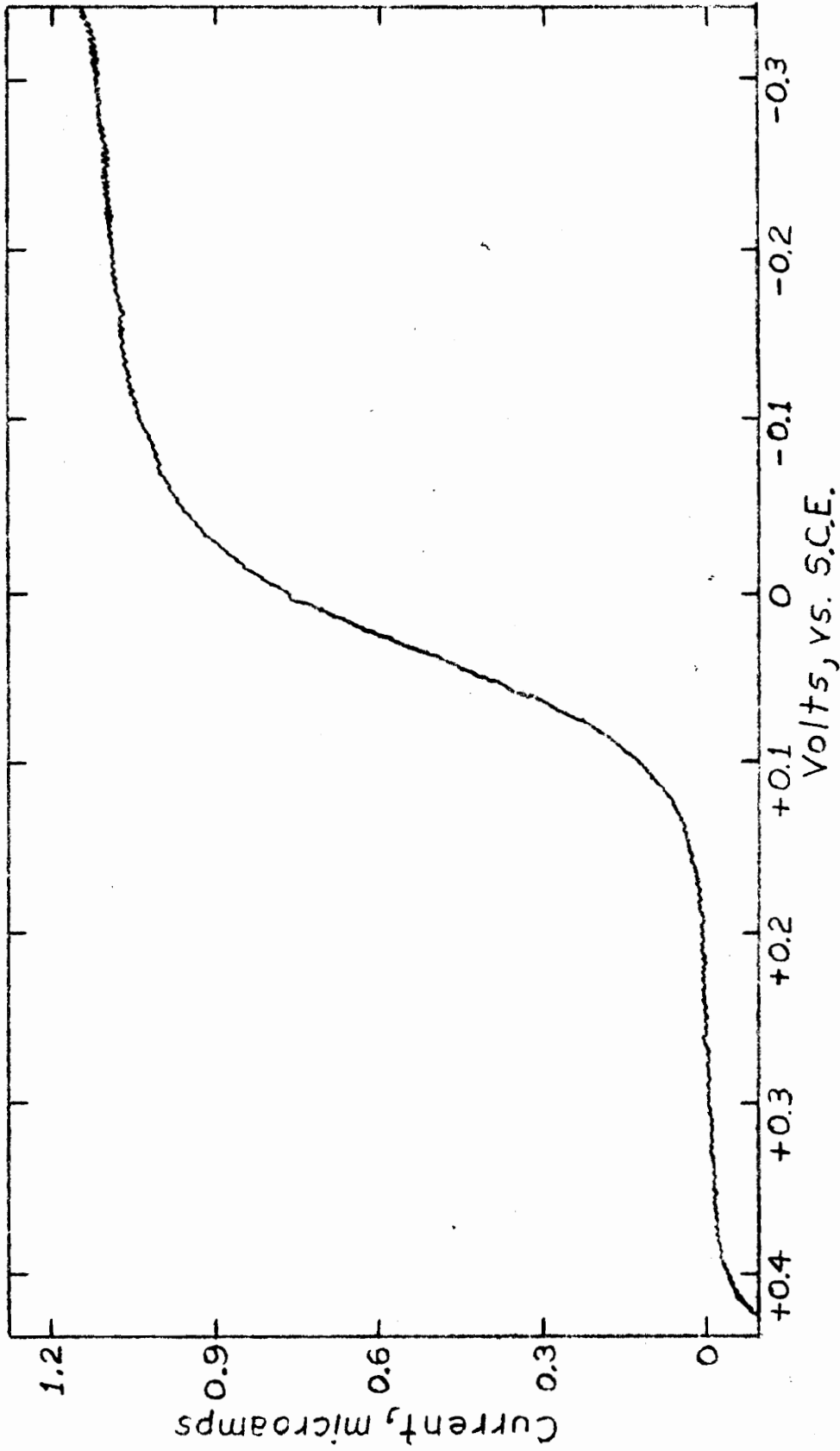
<u>pH</u>	<u>$E_{1/2}$, volts</u>	<u>$i_1, \mu\text{a}$</u>	<u>Slope</u>
6.31	+ 0.035	1.18	0.0711
6.58	+ 0.045	1.24	0.0635
6.93	+ 0.037	1.34	0.0731
6.95	+ 0.040	1.38	0.0610
7.10	+ 0.038	1.13	0.0695
10.50	+ 0.036	1.18	0.0725
11.26	+ 0.037	1.14	0.0753
12.15	+ 0.039	1.13	0.0707

TABLE 17

The Reduction of 0.0001M $[\text{Co}(\text{dipy})_2(\text{NO}_2)_2]\text{Cl}$ as a Function of pH in 0.5M Acetate Buffer at the Rotating Platinum Electrode

<u>pH</u>	<u>$E_{1/2}$, volts</u>	<u>$i_1, \mu\text{a}$</u>	<u>Slope</u>
4.78	+ 0.041	0.39	0.0715
5.13	+ 0.078	0.42	0.0783
5.20	+ 0.040	0.34	0.0735
6.00	+ 0.054	0.44	0.0695
6.17	+ 0.049	0.48	0.0763

Figure 18



Polarogram of the Reduction of $[\text{Co}(\text{dipy})_2(\text{NO}_2)_2]\text{Cl}$
at the Rotating Platinum Electrode in Phosphate Buffer
at pH 12.15

TABLE 18

The Reduction of 0.0002M $[\text{Co}(\text{dipy})_2(\text{C}_2\text{O}_4)]\text{Cl}$ as a Function of pH in 0.5M Phosphate Buffer at the Rotating Platinum Electrode

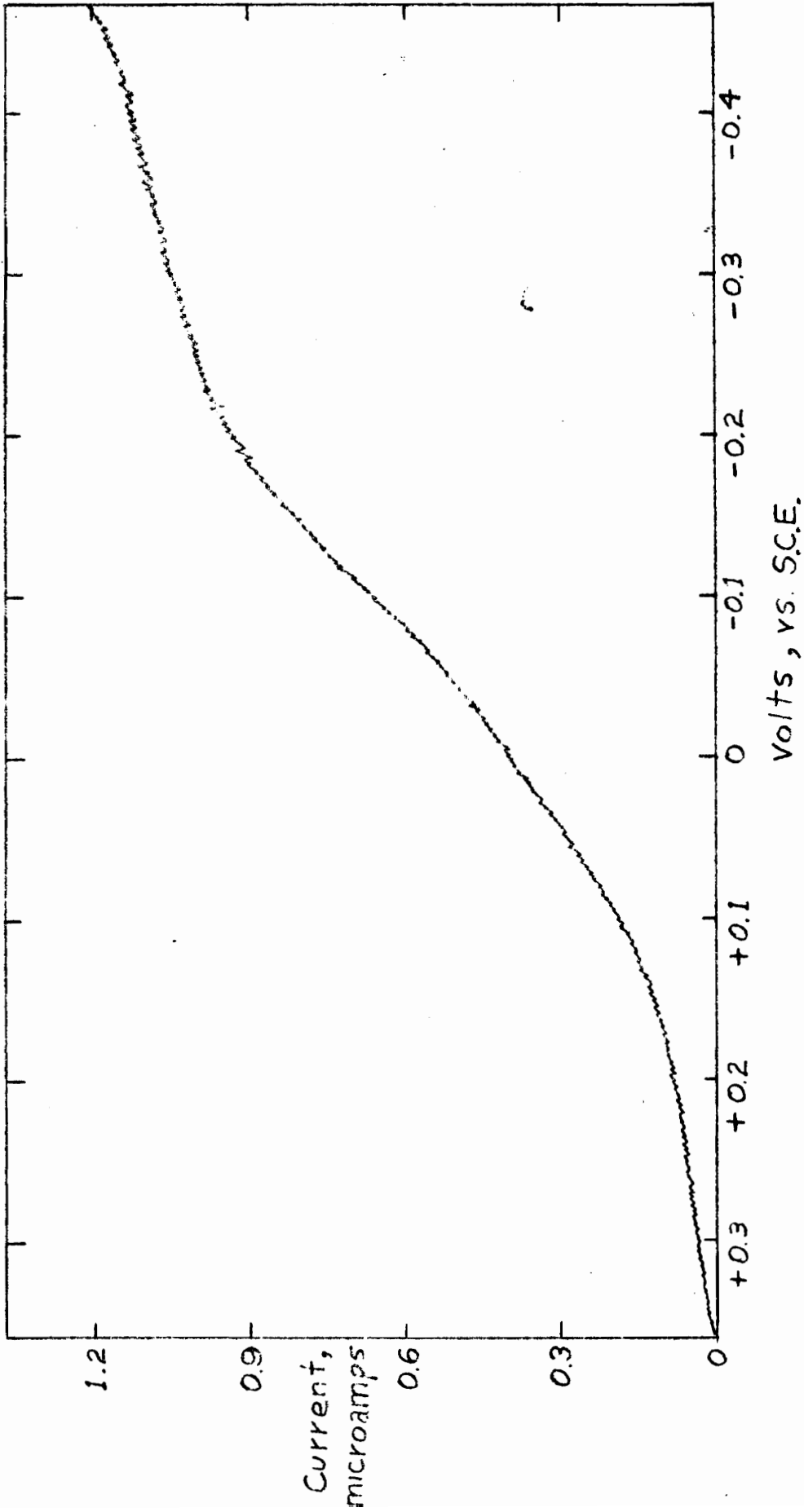
<u>pH</u>	<u>$E_{1/2}$, volts</u>	<u>$i_1, \mu\text{a}$</u>	<u>Slope</u>
5.70	+ 0.017	0.51	0.1035
6.13	+ 0.063	0.66	0.1230
6.43	+ 0.051	0.60	0.1325
8.16	+ 0.053	0.95	0.0865
9.73	+ 0.045	0.50	0.0782
10.60	-0.066	0.78	0.1452

TABLE 19

The Reduction of 0.0001M $[\text{Co}(\text{dipy})_2(\text{C}_2\text{O}_4)]\text{Cl}$ as a Function of pH in 0.5M Acetate Buffer at the Rotating Platinum Electrode

<u>pH</u>	<u>$E_{1/2}$, volts</u>	<u>$i_1, \mu\text{a}$</u>	<u>Slope</u>
2.50	+ 0.006	0.44	0.1335
4.44	+ 0.080	0.38	0.0850
4.73	+ 0.024	0.32	0.0935
5.10	+ 0.045	0.35	0.0812
6.00	+ 0.074	0.32	0.0810

Figure 19



Polarogram of the Reduction of $[\text{Co}(\text{dipy})_2(\text{C}_2\text{O}_4)]\text{Cl}$ at the Rotating Platinum Electrode in Phosphate Buffer at pH 10.60

TABLE 20

The Reduction of 0.001M $[\text{Co}(\text{phen})_2(\text{NO}_2)_2]\text{NO}_3$ as a Function of pH in 0.5M Phosphate Buffer at the Rotating Platinum Electrode

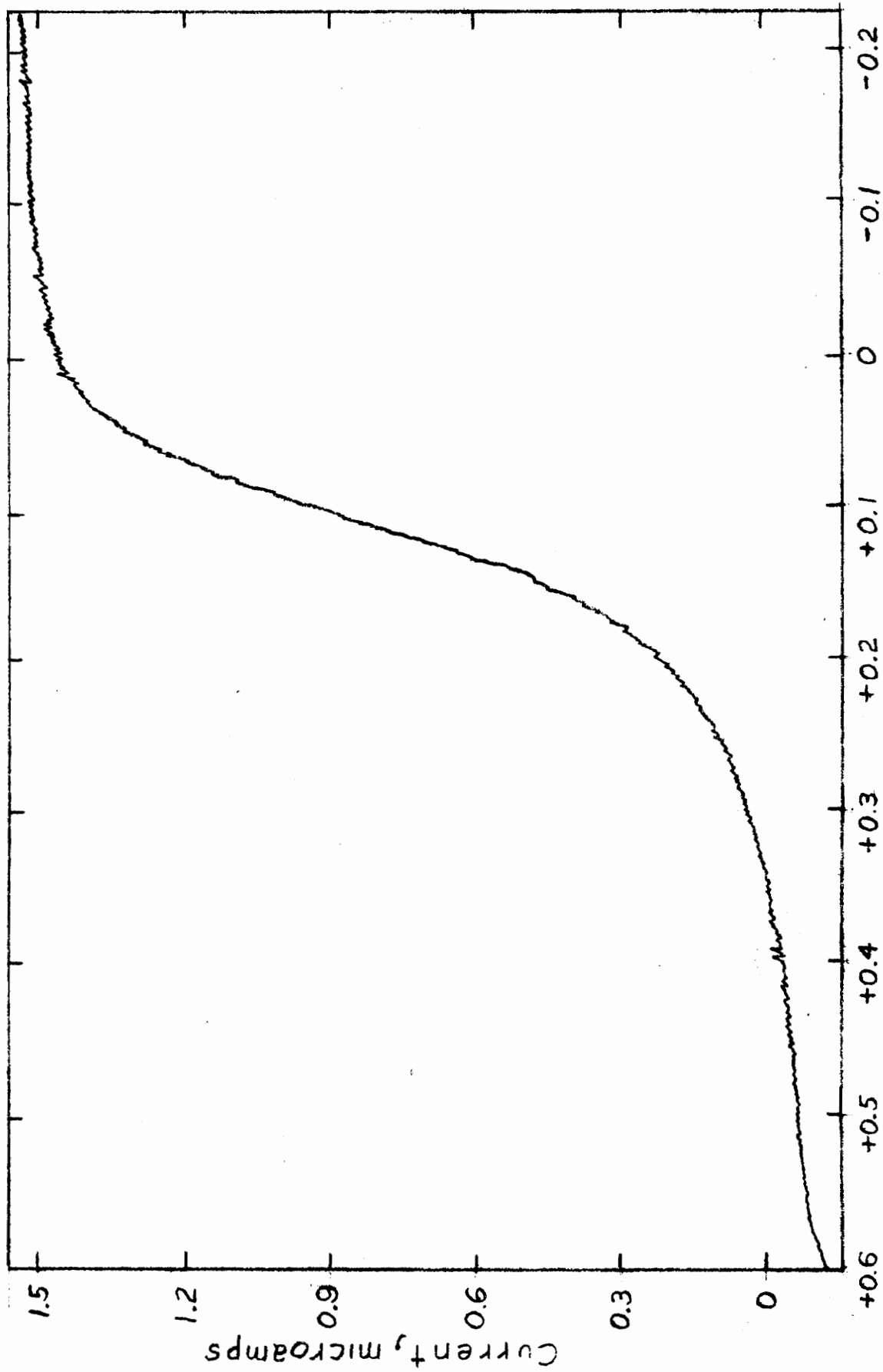
<u>pH</u>	<u>$E_{1/2}$, volts</u>	<u>$i_1, \mu\text{a}$</u>	<u>Slope</u>
6.06	+ 0.120	1.05	0.0915
6.14	+ 0.140	1.46	0.0708
6.34	+ 0.095	1.20	0.1285
6.70	+ 0.095	1.23	0.1045
7.16	+ 0.137	1.50	0.0635
7.41	+ 0.114	0.95	0.0632
7.74	+ 0.119	1.31	0.0697
7.83	+ 0.106	1.30	0.0763
8.36	+ 0.103	1.44	0.0810
9.02	+ 0.103	1.47	0.0875

TABLE 21

The Reduction of 0.001M $[\text{Co}(\text{phen})_2(\text{NO}_2)_2]\text{NO}_3$ as a Function of pH in 0.5M Acetate Buffer at the Rotating Platinum Electrode

<u>pH</u>	<u>$E_{1/2}$, volts</u>	<u>$i_1, \mu\text{a}$</u>	<u>Slope</u>
3.87	+ 0.142	1.69	0.0735
4.19	+ 0.128	1.58	0.1285
4.55	+ 0.113	1.46	0.0949
4.69	+ 0.123	1.63	0.0943
4.87	+ 0.118	1.77	0.0908
5.21	+ 0.117	1.49	0.0849
5.35	+ 0.122	1.45	0.0808
5.46	+ 0.112	1.71	0.0829
5.66	+ 0.112	1.40	0.0703
5.80	+ 0.112	1.44	0.0735

Figure 20



Polarogram of the Reduction of $[\text{Co}(\text{phen})_2(\text{NO}_2)_2]\text{NO}_3$ at the Rotating Platinum Electrode in Phosphate Buffer at pH 7.63

TABLE 22

Comparison of Half Wave Potentials at the Dropping
Mercury Electrode and at the Rotating Platinum Electrode

<u>Compound</u>	<u>$E_{\frac{1}{2}}$ at the Mercury Drop (First Wave), volts</u>	<u>$E_{\frac{1}{2}}$ at the Rotating Platinum Electrode (Avg.), volts</u>
$[\text{Co}(\text{en})_2(\text{NO}_2)_2]\text{NO}_3$	-0.265	-0.543
$[\text{Co}(\text{en})_2(\text{NCS})_2]\text{NCS}$	-0.060	-0.294
$[\text{Co}(\text{en})_2(\text{C}_2\text{O}_4)]\text{Cl}$	-0.316	-0.535
$[\text{Co}(\text{dipy})_2(\text{NO}_2)_2]\text{Cl}$	< 0.100*	+0.038
$[\text{Co}(\text{dipy})_2(\text{C}_2\text{O}_4)]\text{Cl}$	< 0.100*	+0.053
$[\text{Co}(\text{phen})_2(\text{NO}_2)_2]\text{NO}_3$	< 0.100*	+0.113

*No significance due to mercury dissolution.

are shown in Table 22. Values for $E_{1/2}$ at the mercury drop are for the first wave in each case. The values for the $E_{1/2}$ at the platinum electrode are the average value of all determination in each case.

The spectra of each of the complexes was obtained over the range from 350 $m\mu$ to 700 $m\mu$ and the wave length of maximum absorption compared to the $E_{1/2}$ of the reduction wave. The half wave potentials were not in agreement with the spectroscopic series.

EXPERIMENTAL

Apparatus

All polarographic measurements were performed using a Leeds and Northrup Model "E" Electrochemograph. The electrolyses at the dropping mercury electrode were performed using a standard polarographic H-cell with a saturated calomel electrode in one branch of the cell connected to the solution being electrolyzed by an agar-agar salt bridge saturated with KCl. For all measurements, the cell was thermostatted at $25^{\circ} \pm 0.1^{\circ}$ C.

All solutions were outgassed with nitrogen for 20 minutes before each determination. Commercial tank nitrogen was used. The removal of all residual oxygen was performed by passing the nitrogen through a series of three washing towers. The first two towers contained a solution of vanadyl sulfate in H_2SO_4 and lightly amalgamated zinc pellets prepared according to the method of Meites and Meites (29). The third tower contained distilled water to trap any acid suspended in the nitrogen stream.

The polarography using the rotating platinum electrode was performed in a 20 ml. H-cell prepared the same as that used with the dropping mercury electrode. The electrode was rotated using the Sargent Rotator 600 r.p.m. synchronous stirrer. The motor was supported individually from the H-cell to minimize vibration. The platinum surface was first coated with melted cerasin wax. After the wax had cooled and hardened, the top surface of the

electrode was cleaned of wax so that about one-tenth of the total platinum surface was exposed.

All pH measurements were performed using a Beckman Model G pH Meter, standardized with Beckman buffers at pH 7 and 10. The pH of each solution was determined at the time it was to be electrolyzed.

Preparation of Solutions

All solutions to be measured at the dropping mercury electrode were prepared from a stock solution of 0.01M complex which was diluted, one to ten, with the buffer solution. All buffers for pH variations were prepared so that the total ionic strength was 0.2M. The phosphate buffers were 0.2M in phosphate ion. The borate buffers were 0.05M in borate ion and 0.15M in KCl. For the variation of ligand concentration, the total ionic strength was adjusted to 0.3M with KCl. The boric acid used for the preparation of the borate buffers had to be recrystallized to ensure reproducible reduction waves. 0.1M NaOH was used for pH adjustment of all buffer solutions.

For the preparation of the solution to be electrolyzed at the rotating platinum electrode, the buffers were adjusted to 0.5M. The concentration of complex had to be varied whenever a different electrode was used, as each electrode had a slightly different surface area exposed. All polarograms for a series on

one compound were obtained using one electrode. The electrodes had to be changed periodically as the coating tended to loosen after extended operation, thereby exposing more surface area.

Pretreatment of the Platinum Electrode

Several methods of pretreatment of the electrode surface were tried but the best results were obtained by pretreatment similar to that proposed by Ferrett and Phillips (30). The electrode was first partially coated with wax as mentioned above. The electrode was then inserted into a buffer solution without the metal ion. The solution was outgassed with oxygen-free nitrogen for 20 minutes. The circuit was then completed and the potential set at -1.0 volts versus the S.C.E. and the rotation of the electrode started. This anodic polarization of the electrode was continued for 10 minutes, at which time the circuit was broken and the electrode stopped. A portion of the stock solution of the metal ion, which had also been outgassed was then pipetted into the buffer solution. The mixture was then stirred by nitrogen bubbling for one minute and the solution electrolyzed immediately. The whole procedure was carried out with a nitrogen atmosphere above the solution.

Characteristics of the Mercury Drop

The dropping mercury electrode used in these determinations had the following characteristics: mass of the drop, 14.62 mg/sec; drop time, 2.80 sec. The drop constant was $7.07 \text{ mg}^{2/3} \text{ sec}^{-1/2}$. The height of the mercury column was held at a constant 30.0 cm for all determinations.

Preparation of Compounds

A series of eight compounds with a bis-diamine cobalt nucleus were prepared, with the remaining coordination positions filled by various negative ligands. The compounds prepared were: trans-dinitro-bis (ethylenediamine) cobalt (III) nitrate, trans-dinitro-bis (1, 10 phenanthroline) cobalt (III) nitrate, trans-dinitro-bis (α, α' dipyridyl) cobalt (III) chloride, cis-dithiocyanato-bis (ethylenediamine) cobalt (III) thiocyanate, oxalato-bis (ethylenediamine) cobalt (III) chloride, oxalato-bis (α, α' dipyridyl) cobalt (III) chloride, sodium bromo-ethylenediaminetetraaceto cobaltate (III), and sodium nitro-ethylenediaminetetraacetato cobaltate (III).

The compounds were prepared as follows:

1. trans-Dinitro-bis-(ethylenediamine) cobalt (III) nitrate.

This compound was prepared by the method set forth in Inorganic Synthesis ⁽²¹⁾: 7.13 g. of 70% ethylenediamine was mixed with 10 ml. water and 3 ml. concentrated HNO_3 . This mixture was

added to a solution of 11.5 g. of $\text{Co}(\text{NO}_3)_2 \cdot 6\text{H}_2\text{O}$ and 6.0 g. of NaNO_2 in 20 ml. water. The compound was oxidized by bubbling air through the solution for twenty minutes. The precipitate which formed was filtered and washed with cold water. The precipitate was dissolved in hot water and recrystallized twice by cooling on an ice bath. The resulting orange crystals were dried in air on the filter paper.

Formula - $[\text{Co}(\text{en})_2(\text{NO}_2)_2]\text{NO}_3$. Analysis calculated: C 14.66, N 29.39 and H 4.34. Found: C 14.43, N 29.45 and H 4.84.

2. trans-Dinitro-bis-(1, 10-phenanthroline) cobalt (III) nitrate. This compound was prepared by a method analogous to that of $[\text{Co}(\text{en})_2(\text{NO}_2)_2]\text{NO}_3$; 0.9 g. of 1,10-phenanthroline was dissolved in 20 ml. of 0.025M HNO_3 . This was then added to a solution of 0.719 g. $\text{Co}(\text{NO}_3)_2 \cdot 6\text{H}_2\text{O}$ and 0.373 g. NaNO_2 in 20 ml. water. No air bubbling was needed as gently boiling for 10 minutes was sufficient for oxidation. The solution was cooled, filtered and recrystallized twice from hot water.

Formula - $[\text{Co}(\text{phen})_2(\text{NO}_2)_2]\text{NO}_3 \cdot \text{H}_2\text{O}$. Analysis calculated: C 48.70, N 16.55 and H 3.08. Found: C 48.25, N 15.63 and H 3.25.

3. (a) cis-Dinitro-bis-(α, α' -dipyridyl) cobalt (III) chloride. This compound was prepared by the method of Jaeger and vanDyk (22): In a solution of 4.762g. $\text{CoCl}_2 \cdot 6\text{H}_2\text{O}$ in 25 ml. water, 6.24 g. dipyridyl were dissolved. 40 ml. of 10% H_2O_2 were then

added with constant stirring. After the reaction had taken place, the dark brown solution was heated on a steam bath. 75 ml. of conc. HCl were then added to produce the green trans-dichlorobis-~~bis~~-(α,α' dipyridyl)cobalt (III) chloride. The solution was concentrated to syrup on a steam bath. The green and purple crystals were dried in a dessicator over CaO. After drying, the crystals were extracted with absolute alcohol, the violet cis-salt being more soluble in alcohol than the green trans isomer. The absolute alcohol solution of the violet salt was cooled on an ice bath to crystallize out the cis-dichlorobis(α,α' dipyridyl)cobalt (III) chloride as the dihydrate. The yield was increased by further addition of conc. HCl to the solution of the green trans isomer and evaporating to syrup again to convert it to the cis isomer.

3. (b) Conversion to the cis dinitro compound: The cis- $[\text{Co}(\text{dipy})_2\text{Cl}_2]\text{Cl}$ was dissolved in hot water. Two equivalents of NaNO_2 were added and the solution was boiled gently for 20 minutes. The solution was cooled in an ice bath to crystallize out the yellow crystals. The crystals were filtered, washed with absolute alcohol and then recrystallized twice from hot water.

Formula - $[\text{Co}(\text{dipy})_2(\text{NO}_2)_2]\text{Cl}\cdot 4\text{H}_2\text{O}$. Analysis calculated:
C 41.95, N 14.70 and H 4.23. Found C 41.13, N 9.23 and H 3.55.

4. Oxalato-bis(ethylenediamine)cobalt (III) chloride.

(a) Preparation of trans-[Co(en)₂(Cl)₂]Cl⁽²³⁾: 600 g.

of 10% ethylenediamine in water were added, with stirring, to 160 g. of CoCl₂·6H₂O in 500 ml. water. Air was bubbled through the solution for 12 hours, then 350 ml. conc. HCl were added. The volume was reduced, on a steam bath, to syrup. On standing green crystals precipitated. The precipitate was filtered and washed with absolute alcohol and ether and dried at 110° C. to drive off excess HCl. The dull green powder resulting was trans-[Co(en)₂(Cl)₂]Cl.

(b) Conversion to cis-dichloro^{bis}(ethylenediamine)cobalt chloride: A neutral solution of the green trans isomer was evaporated to dryness on a steam bath. The resulting purple crystals of cis-[Co(en)₂(Cl)₂]Cl were purified by washing with small amounts of water. The more soluble trans isomer which is dissolved out may be converted to the cis isomer by additional evaporations to dryness. No more than three evaporations were done, as the compound is degraded by continued heating. The cis compound was not dried, as it would be used only for conversion to the oxalato form.

(c) Conversion to Oxalato-bis(ethylenediamine)cobalt (III) chloride: to a solution of 6.04 g. of cis [Co(en)₂(Cl)₂]Cl in 50 ml. water, a solution of 2.68 g. sodium oxalate in 25 ml.

of 0.4M HNO₃ was added. The mixture was boiled slowly for 10 minutes, then cooled on an ice bath and filtered. The resulting bright red crystals of $[\text{Co}(\text{en})_2(\text{C}_2\text{O}_4)]\text{Cl}$ were purified by recrystallization from hot water.

Formula - $[\text{Co}(\text{en})_2(\text{C}_2\text{O}_4)]\text{Cl}$. Analysis calculated: C 23.80, N 18.50 and H 5.43. Found: C 21.96, N 18.26 and H 5.45.

5. Oxalato-bis-(α, α' -dipyridyl) cobalt (III) chloride.

Starting with $\text{cis-}[\text{Co}(\text{dipy})_2(\text{NO}_2)_2]\text{Cl}$ prepared by the method given above, 4.99 g. were dissolved in 50 ml. water. To this was added a solution of 0.535 g. NH₄Cl in 20 ml. water. This was then boiled gently for 30 minutes, a solution of 1.34 g. Na₂(C₂O₄) in 50 ml. water was added, and the volume was reduced to 50 ml. on a steam bath. The solution was cooled in an ice bath, and the resulting red-orange crystals were purified by twice recrystallizing from hot water.

Formula - $[\text{Co}(\text{dipy})_2(\text{C}_2\text{O}_4)]\text{Cl} \cdot 2\text{H}_2\text{O}$. Analysis calculated: C 49.75, N 10.54 and H 3.89. Found: C 46.88, N 10.22 and H 2.87.

6. Cis-dithiocyanato-bis-(ethylenediamine) cobalt (III) thiocyanate. This compound was prepared from $\text{trans-}[\text{Co}(\text{en})_2(\text{NO}_2)_2]\text{NO}_3$ by the method of Ablov and Lobanov (24). 3.0 g. $[\text{Co}(\text{en})_2(\text{NO}_2)_2]\text{NO}_3$ and 10 g. NH₄NCS were dissolved in 50 ml. water, and heated slowly to boiling. When the reaction had ceased, the solution was concentrated on a steam bath, then cooled to crystallize out the red $[\text{Co}(\text{en})_2(\text{NCS})_2]\text{NCS}$.

Formula - $\text{cis-}[\text{Co}(\text{en})_2(\text{NCS})_2]\text{NCS}$. Analysis calculated:
C 23.75, N 27.73 and H 4.57. Found: C 21.32, N 28.03 and H 4.70.

7. Sodium bromo-ethylenediamine tetraaceto cobaltate (III).

This compound was prepared by the method of Schwarzenbach⁽²⁵⁾. To a solution of 23.8 g. $\text{CoCl}_2 \cdot 6\text{H}_2\text{O}$ was added a solution of 37.2 g. disodium ethylenediaminetetraacetate dihydrate. The solution was heated to boiling. When the reaction was complete, the solution was cooled and an excess of bromine water was added. A few drops of HNO_3 were added. When this reaction subsided, enough HNO_3 was added to give a pH of about 1.0. At this point, blue-green crystals precipitate. The crystals were filtered and washed with 0.1M HNO_3 . The compound was dried in air as the dihydrate.

Formula - $\text{Na}[\text{Co}(\text{EDTA})\text{Br}] \cdot 2\text{H}_2\text{O}$. Analysis calculated: C 24.57, N 5.74, and H 3.51. Found: C 25.43, N 5.65 and H 4.10.

8. Sodium nitro-ethylenediaminetetraaceto cobaltate (III).

This compound was prepared from the $\text{Na}[\text{Co}(\text{EDTA})\text{Br}]$. The bromo compound was dissolved in a solution of sodium acetate. The solution was then made slightly acidic with acetic acid. A solution of Hg^{2+} , 0.5 moles Hg^{2+} per mole of compound, was added to extract Br^- from the coordination sphere. A slight excess of Hg^{2+} was added to assure complete reaction, and the HgBr_2 was filtered off. 1.0 mole of NaNO_2 , per mole of compound, was then added then acid was added until a precipitate formed.

The solution was cooled in an ice bath and the resulting $\text{Na}[\text{Co}(\text{EDTA})\text{NO}_2]$ was filtered. The compound was dried in air as the dihydrate.

Formula - $\text{Na}[\text{Co}(\text{EDTA})\text{NO}_2] \cdot 2\text{H}_2\text{O}$. Analysis calculated:
C 26.50, N 9.28 and H 3.78. Found C 26.27, N 9.23 and H 4.05.

All compounds were prepared by standard methods. The discrepancy in the nitrogen analysis of the cis dinitro-bis (α, α' dipyridyl) cobalt (III) chloride may be accounted for by the excessive amount of residue reported for the analysis of this compound.

CONCLUSIONS

The observations of Mason⁽³¹⁾ were duplicated, with respect to the reversibility of the first reduction wave $[\text{Co}(\text{en})_2(\text{NO}_2)_2]\text{NO}_3$. The shift observed in the $E_{1/2}$ of the first wave, with nitrite ion, of 0.060 volts per 10 fold change in nitrite ion concentration, indicate that one nitrite is released as a part of the primary electrode process. The release of one nitrite upon reduction, suggests the formation of either an aquo complex or a five-coordinated complex of the type suggested by Adamson⁽³³⁾ and Nyholm⁽³⁴⁾.

Establishing a mechanism for the electrode process of the first wave of the $[\text{Co}(\text{en})_2(\text{NCS})_2]\text{NCS}$ and $[\text{Co}(\text{en})_2(\text{C}_2\text{O}_4)]\text{Cl}$ is complicated by the irreversibility of the wave. However, the data does indicate that the primary electrode process does involve the release of a ligand, after which the complex decomposes to some species with a $[\text{Co}(\text{en})_2]^{2+}$ base and finally, in solutions sufficiently alkaline, the formation $[\text{Co}(\text{en})_3]^{2+}$.

The second wave of all three ethylenediamine complexes may be attributed to the oxidation of this tris-ethylenediamine cobalt (II) species.

The ortho-phenanthroline complex, the two dipyridyl complexes and the two ethylenediamine-tetraacetate complexes all show reduction waves too positive to be free from interference from the mercury anodic wave at the mercury drop. The data obtained

from the orthophenanthroline and the two dipyridyl complexes at the platinum electrode does indicate the relative stabilities of the complexes.

The irreversible behavior, even for $[\text{Co}(\text{en})_2(\text{NO}_2)_2]\text{NO}_3$, at the platinum electrode is probably due to stirring of the solution which would remove the products of the electrode reaction from the electrode surface as fast as they formed, so that diffusion control of the reactions was not established.

BIBLIOGRAPHY

1. Taube, H., *Chem. Rev.*, 50, 69, (1952).
2. Tsuchida, R., Et al., *Bull. Chem. Soc. Japan*, 30, P. 909, (1957).
3. Holtzclaw, H. F., and Sheetz, D. P., *J. Am. Chem. Soc.*, 75, 3053, (1953).
4. Adamson, A. W., *ibid.*, 78, 4260, (1956).
5. Laitinen, H. A. and Grieb, M. W., *ibid.*, 77, 5201, (1955).
6. Kivalo, P., *ibid.*, 77, 2678, (1955).
7. Dolezal, J., *Chem. Listy*, 49, 1017, (1955), *C. A.*, 49, 14533, (1955).
8. Gillespie, R. J., and Nyholm, R. S., "Progress in Stereochemistry" Edited by W. Klyne and P. B. D. de la Mare, Vol. 2, p. 300, Butterworth Scientific Publications, London, 1958.
9. Mason, J. G., Paper Presented before the Phys. Chem. Section of the Am. Chem. Soc. Meeting, Chicago, Illinois, 1958.
10. Marcus, R. A., *J. Chem. Phys.*, 26, 857, (1957).
11. Irvine, D. H., *J. Chem. Soc.*, 2977, (1959).
12. Taube, H., "Inorganic and Radiochemistry," Edited by H. G. Emeleus and A. G. Sharpe, Vol. 1, Ch. 1, Academic Press, Inc., New York, N. Y., (1959).
13. Laitinen, H. A. and Kivalo, P., *J. Am. Chem. Soc.*, 75, 2198, (1953).
14. Kivalo, P., reference 6 above.
15. Laitinen, H. A. and Grieb, M., reference 5 above.
16. Holtzclaw, H. F. and Sheetz, D. P., reference 3 above.
17. Mason, J. G., reference 9 above.
18. Vlcek, A. A., *Disc. Faraday Soc.*, No. 26, 164, (1958).

19. Tsuchida, R., Bull. Chem. Soc. Japan, 32, 150 (1959), C. A. 53, 2885 (1959).
20. Hume, D. N. and Kolthoff, I. M., J. Am. Chem. Soc., 71, 867, (1949).
21. Holtzclaw, H. F., Jr., Sheetz, D. P., and McCarty, B. D., "Inorganic Synthesis," Vol. IV, p. 179, John Wiley and Sons, New York, N. Y., (1953).
22. Jaeger, F. M. and VanDyk, A., Z. anorg. allgem. Chem., 227, 317, (1936).
23. Holtzclaw, H. F., Sheetz, D. P., and McCarty, B. D., "Inorganic Synthesis," Vol. IV, John Wiley and Sons, New York, N. Y., 1953.
24. Ablov, A. V. and Lobanov, N. I., J. Inorg. Chem. (Russian) 4, 149 (1959).
25. Schwarzenbach, G., Helv. Chem. Acta., 32, 839, (1949).
26. Heyrovsky, J., Chem. Listy, 16, 256, (1922).
27. Heyrovsky, J. and Shikata, M., Rec. trav. chem. 44, 496, (1925).
28. Kolthoff, I. M. and Laitinen, H. A., Science, 92, 152, (1940).
29. Meites, L. and Meites, T., Anal. Chem., 20, 984, (1948).
30. Ferrett, D. J., and Phillips, C.S.G., Tran. Faraday Soc., 51, 390, (1955).
31. Mason, J. G., reference 9 above.
32. Laitinen, H. A. and Kivalo, P., reference 13 above.
33. Adamson, A. W., reference 4 above.
34. Gillespie, R. J. and Nyholm, R. S., reference 8 above.

VITA

Richard Lee White was born in Sharon, West Virginia, on March 8, 1934.

He graduated from East Bank High School, East Bank, West Virginia, in June 1951. He entered West Virginia Institute of Technology in September of the same year, and completed the requirements for the degree of Bachelor of Science in Chemistry in June, 1956.

From June, 1956, until July, 1959, he was employed by the American Electric Power Company as a power plant chemist.

In July, 1959, he entered the Virginia Polytechnic Institute pursuant to a Masters degree in chemistry.

From March, 1961, until the present time, he has been employed by Hercules Power Company, at Radford Ordnance Plant as a Process Engineer.

Richard Lee White

ABSTRACT

A series of eight compounds with bis-diamine cores were prepared and their electrochemical behavior explored polarographically. The behavior of the compounds was studied at the dropping mercury electrode and the rotating platinum electrode.

Trans-dinitro-bis-(ethylenediamine) cobalt (III) nitrate shows reversible behavior in well buffered solutions at the dropping mercury electrode. The mechanism for the reduction is proposed as; rapid, reversible electron transfer; decomposition of the reduced species; and, in solutions sufficiently alkaline, the formation of tris-(ethylenediamine) cobalt (II), thereby accounting for the observed second wave.

The reduction of cis dithiocyanato-bis-(ethylenediamine) cobalt (III) thiocyanate and oxalato-bis-(ethylenediamine) cobalt (III) chloride both give irreversible waves, thereby complicating any proposal of a mechanism. The observed second reduction wave, though, appears to be caused by the formation of tris-(ethylenediamine) cobalt (II), as in the case of the dinitro compound.

A proposal of the mechanism for the other five compounds was not possible as they either reduced at too positive a potential, aquated too rapidly, or both.